THESIS – TM 185400

MECHANICAL MODELING AND CONTROL OF SUSPENDED CABLE DRIVEN PARALLEL ROBOT (CDPR) FOR SEARCH AND RESCUE OPERATION

ADLINA TAUFIK SYAMLAN
02111850080010

Supervisor
Ir. Bambang Pramujati, M.Sc.Eng, Ph.D.
Latifah Nurahmi, S.T., M.Sc., Ph.D.

Mechanical Engineering Department
Faculty of Industrial and Systems Engineering
Institut Teknologi Sepuluh Nopember
2020

THESIS – TM 185400

MECHANICAL MODELING AND CONTROL OF SUSPENDED CABLE DRIVEN PARALLEL ROBOT (CDPR) FOR SEARCH AND RESCUE OPERATION

ADLINA TAUFIK SYAMLAN
02111850080010

Supervisor
Ir. Bambang Pramujati, M.Sc.Eng, Ph.D.
Latifah Nurahmi, S.T., M.Sc., Ph.D.

Mechanical Engineering Department
Faculty of Industrial and Systems Engineering
Institut Teknologi Sepuluh Nopember
2020

TESIS – TM 185400

MODEL MEKANIS DAN KONTROL DARI *SUSPENDED CABLE DRIVEN PARALLEL ROBOT* (CDPR) UNTUK OPERASI PENCARIAN DAN PENYELAMATAN

ADLINA TAUFIK SYAMLAN
02111850080010

Dosen Pembimbing
Ir. Bambang Pramujati, M.Sc.Eng, Ph.D.
Latifah Nurahmi, S.T., M.Sc., Ph.D.

Departemen Teknik Mesin
Fakultas Teknologi Industri dan Rekayasa Sistem
Institut Teknologi Sepuluh Nopember
2020

LEMBAR PENGESAHAN TESIS

Tesis disusun untuk memenuhi salah satu syarat memperoleh gelar

Magister Teknik (M.T.)

di

Institut Teknologi Sepuluh Nopember

oleh:

Adlina Taufik Syamlan

NRP: 02111850080010

Tanggal Ujian: 23 Juni 2020

Periode Wisuda: September 2020

Disetujui Oleh:

Pembimbing:

1. Ir. Bambang Pramujati, M.Sc.Eng, Ph.D
   196912031994031001 .....
2. Latifah Nurahmi, S.T., M.Sc., Ph.D.
   NIP. 1986201712037 .....

Penguji:

1. Prof. Ir. I Nyoman Sutantra, MSc., Ph.D
   NIP. 195106051978031002 .....
2. Dr. Eng. Unggul Wasiwitono, ST., M.Eng., Sc.
   NIP. 197805102001121001 .....

Kepala Departemen Teknik Mesin

Fakultas Teknologi Industri dan Rekayasa Sistem

Dr.Ir.Atok Setiyawan, M.Eng.Sc.

NIP. 196604021989031002

THESIS APPROVAL SHEET

This thesis is written to fulfill one of the prerequisites in obtaining the following degree

Magister Teknik (M.T.)

at

Institut Teknologi Sepuluh Nopember

by:

Adlina Taufik Syamlan

NRP: 02111850080010

Date of Examination: June 23rd, 2020

Graduation Period: September 2020

Approved by:

Supervisors:

1. Ir. Bambang Pramujati, M.Sc.Eng, Ph.D
   196912031994031001 .....
2. Latifah Nurahmi, S.T., M.Sc., Ph.D.
   NIP. 1986201712037 .....

Examiners:

1. Prof. Ir. I Nyoman Sutantra, MSc., Ph.D
   NIP. 195106051978031002 .....
2. Dr. Eng. Unggul Wasiwitono, ST., M.Eng., Sc.
   NIP. 197805102001121001 .....

Head of Mechanical Engineering Department

Faculty of Industrial Technology and System Engineering

Dr.Ir.Atok Setiyawan, M.Eng.Sc.

NIP. 196604021989031002

MECHANICAL MODELING AND CONTROL OF SUSPENDED CABLE DRIVEN PARALLEL ROBOT (CDPR) FOR SEARCH AND RESCUE OPERATION

Name : Adlina Taufik Syamlan

NRP : 02111850080010

Supervisor : Ir. Bambang Pramujati, M.Sc.Eng, Ph.D.

Latifah Nurahmi, S.T., M.Sc., Ph.D

ABSTRACT

Indonesia sits in the natural disaster-prone zone, named the ring of fire. The ring is home to the strongest recorded volcanic and seismic activities on earth. On such events, the sheer amount of energy released can destroy buildings, risking of victims being trapped inside. The current search – and – rescue operation relies heavily on manual labor and heavy machinery. Both have limited power and mobility. This hindrance slows the rescue process, increasing the fatality rate. Therefore, a solution that combines both mobility and power is needed to aid the process. One of the alternatives is by using a Cable-Driven Parallel Robot (CDPR). This research aims to develop a CDPR for search and rescue robot in terms of its dynamic behavior and control system.

This research introduces a suspended CDPR which consists of 4 cables attached to the top sides of a cube fix frame in one end, and a cube moving platform at another end. Each cable is guided by reconfigurable pulleys and is actuated by a stepper motor at the bottom side of the fixed frame. Each motor is equipped with a winch. The objective of this research is to observe the behavior of CDPR under a dynamic trajectory, under the influence of pulley mechanisms with two sets of cable arrangements. With each cable arrangement, the robot will be simulated through three trajectories to find tension distributions, along with the angles, errors, and velocity. This knowledge is then used to design a suitable control scheme (termed

model-based control). It is simulated to see the response and to see whether a compensator is required (termed error compensation control). Due to complexity, the reconfigurability is not displayed.

It is observed that the reconfigurable pulleys can ensure the dynamic feasibility of the robot. The ability of CDPR to follow dynamic trajectory is significantly improved, especially for the standard cable arrangement. An almost identical result is seen between fixed and reconfigurable pulleys when using crossing cable arrangement. As for its control scheme, in general, the model-based control scheme performs better in both x and y-axis, but not in the z-axis. The error compensation scheme can perform better than the model-based ones, reducing error for all trajectories, noticeably in the z-axis.

Keywords: cable robot, reconfigurable pulleys, kinematic, robot control, dynamic, trajectory planning, search – and rescue

MODEL MEKANIS DAN KONTROL DARI *SUSPENDED CABLE DRIVEN PARALLEL ROBOT (CDPR)* UNTUK OPERASI PENCARIAN DAN PENYELAMATAN

Nama : Adlina Taufik Syamlan

NRP : 02111850080010

Pembimbing : Ir. Bambang Pramujati, M.Sc.Eng, Ph.D.

Latifah Nurahmi, S.T., M.Sc., Ph.D

ABSTRAK

Indonesia berada di zona rawan bencana alam, dinamai *ring of fire*. Daerah ini adalah daerah dengan aktivitas vulkanik dan seismik terkuat di bumi. Saat bencana alam terjadi, banyaknya energi yang dilepaskan dapat menghancurkan gedung-gedung, sehingga banyak korban yang dapat terperangkap di dalam. Operasi pencarian dan penyelamatan saat ini sangat bergantung pada manusia dan mesin berat, yang keduanya memiliki kekuatan dan mobilitas yang terbatas. Hal ini memperlambat proses penyelamatan, sehingga tingkat kematian meningkat. Oleh karena itu, solusi yang menggabungkan mobilitas dan kekuatan diperlukan untuk membantu proses tersebut. Salah satu alternatif solusi dari masalah ini adalah dengan menggunakan Cable-Driven Parallel Robot (CDPR). Penelitian ini bertujuan untuk mengembangkan CDPR untuk robot pencarian dan penyelamatan dalam hal perilaku dinamis dan sistem kontrol.

Penelitian ini memperkenalkan CDPR yang terdiri dari 4 kabel menghubungkan rangka *fixed cube* di satu ujung, dan *cube platform* yang bergerak di ujung lainnya. Setiap kabel melewati katrol yang dapat dikonfigurasi ulang dan terhubung ke motor *stepper* sebagai penggerak dan terletak di setiap sisi bawah rangka *fixed cube*. Setiap motor dilengkapi dengan *winch*. Tujuan dari penelitian ini adalah untuk mengamati perilaku CDPR di bawah trajektori dinamis, di bawah pengaruh mekanisme katrol dengan dua set susunan kabel. Untuk setiap susunan

kabel, robot akan disimulasikan melalui tiga trajektori untuk mendapatkan distribusi tegangan, sudut, *error*, dan kecepatan kabel. Pengetahuan ini kemudian digunakan untuk merancang skema kontrol yang cocok (dinamakan *model-based*). Kontrol tersebut disimulasikan untuk melihat respons dan apakah kompensator diperlukan (disebut *error – compensation*). Untuk tahap awal, konfigurasi ulang katrol tidak ditampilkan.

Dari simulasi, terlihat bahwa katrol yang dapat dikonfigurasi ulang dapat memastikan kelayakan dinamis robot. Kemampuan CDPR untuk mengikuti trajektori dinamis meningkat secara signifikan, terutama untuk susunan kabel standar. Hasil yang hampir identik terlihat antara katrol yang tetap dan yang dikonfigurasi ulang saat menggunakan susunan kabel silang. Adapun skema kontrolnya, secara umum, skema kontrol *model-based* berperforma lebih baik di sumbu x dan y, tetapi tidak di sumbu z. Skema *error compensation* menghasilkan kinerja lebih baik daripada menggunakan *model – based*, dengan mengurangi kesalahan untuk semua lintasan, terutama pada sumbu z.

Kata Kunci: *cable robot*, konfigurasi ulang katrol, kinematika, kontrol robot, dinamika, perencanaan trajektori, trajectory planning, pencarian dan penyelamatan

FOREWORD

The author would like to thank the Ministry of Research and Higher Education of Indonesia as funder of this research, under the scheme of Internal Collaboration Research 2018–2020, with title *Contoller Design and Dynamics Analysis of a Search and Rescue Cable Driven Parallel Robot*.

The author would also like to share her deepest gratitude to Ir. Bambang Pramujati, M.Sc.Eng, Ph.D and Latifah Nurahmi, S.T., M.Sc., Ph.D, for their supervision and guidance in this project, along with Mohamad Nasir Tamara, M.T. as supervisor in the constuction of the prototype.

(This page is left intentionally blank)

TABLE OF CONTENTS

(This page is left intentionally blank)

LIST OF FIGURES

LIST OF TABLES

(This page is left intentionally blank)

CHAPTER 1

INTRODUCTION

1.1. Background

Indonesia sits in the natural disaster-prone zone, named the ring of fire. The ring is home to the strongest recorded volcanic and seismic activities on earth. On such events, the sheer amount of energy released can destroy buildings, risking of victims being trapped inside, the current search – and – rescue operation relies heavily on manual labor and heavy machinery. Both have limited power and mobility. This hindrance slows the rescue process, increasing the fatality rate. Therefore, a solution that combines both mobility and power is needed to aid the process, which is Cable-Driven Parallel Robot (CDPR).

The main advantages of using CDPR are big workspaces and easy setups. This unique ability is perfect for remote regions and will improve the evacuation process significantly. Since cables are flexible, they can be easily coiled and uncoiled, thus gives bigger workspaces (Gosselin, 2013). Furthermore, the cables can be easily connected and disconnected to the moving platform. By adopting cables instead of rigid links leads to a significant reduction of moving masses. Although the CDPR are lightweight structures, their payload capability is quite high because the payload is distributed among cables (Qian et al., 2018). Consequently, they can handle heavy loads, like the crane, and can achieve high accelerations and velocities

1.2. Problem Statement

Problem statement for this research are as follows:

1. How are the derivations on geometric, dynamic, and kinematic analysis concerning pulley mechanisms on the CDPR?
2. How are the dynamic behaviors of the CDPR in terms of tension distribution and velocity?
3. What is the suitable control scheme for controlling the CDPR?

1.3. Scope of the Problem

The scope of the problems is limited to, along with assumptions as follows:

1. The robot is constructed to have 3-DOF Translation only
2. Cables are assumed rigid and massless
3. Winches are assumed ideal, meaning that it will always coil one layer of cables
4. Transmission loss within the actuator is assumed negligible
5. Pulley mass and friction between pulley and cable are assumed negligible
6. The reconfigurable pulleys will not be in cooperated in the control scheme due to the complexity of the algorithm which cannot be applied in real-time.
7. The control scheme is designed to control position only
8. No missed steps occurred in the stepper motor

1.4. Problem Objectives

The objectives of this research project are as follows:

1. Derive geometric, dynamic, and kinematic analysis while considering the influence of pulleys
2. Analyze the dynamic equilibrium of the CDPR in terms of its tension distribution and velocity.
3. Construct a suitable control scheme of the CDPR, concerning the design requirements.

1.5. Significance and Contribution of the Research

The significance of the research is both in the kinematic analysis and its control scheme of the CDPR. Reconfigurability of CDPR has been the focus within the past 5 years but focusing on the reconfigurable exit points. This research focuses on the reconfigurability of the pulleys and taking into account its mechanism, in which to the author's knowledge has not been done.

Also, most of the developed control schemes use sensors to estimate cable length. To the author's knowledge, this is done by gathering data from the encoder. The encoder reads rotations generated by a servo motor. This research approaches this differently by using stepper motors instead of servos. By using stepper motors, sensors are not needed since it moves in a discrete number of steps.

(This page is left intentionally blank)

CHAPTER 2

LITERATURE REVIEW AND THEORETICAL BACKGROUND

2.1. State of the Art

The development of a parallel manipulator for universal tire testing by Van Gough of Dunlop Tires marks the start of research on parallel manipulators in the early 1950s (Gough and Whitewall, 1962). One of the new types of manipulators that were developed is termed Cable-Driven Parallel Robot. It gained interest among researchers due to its potential applications. The mechanical properties possessed by the cables such as high payload, along with the coil-uncoil nature of cables (Qian et al., 2018) can expand the workspace considerably (Gosselin, 2013) which fits perfectly in vast amount real-world application including search-and-rescue operations (Caro and Martin, 2016). Examples of well-known prototypes are IPAnema (Pott, et al., 2013) and CoGiRo (El-Ghazaly et al., 2014), as shown in Figure 2.1 and Figure 2.2 respectively.

Figure 2.1. (a)IPAnema 1 and (b)IPAnema 2 (Pott, et al., 2013)

Figure 2.2. CoGiRo (El-Ghazaly et al., 2014)

The earliest work on wire robot dates back in 1988, intended for Skycam (Tanaka et al., 1988). Within the same year, ROBOCRANE from the National Institute of Standards and Technology (NSIT) has also been developed. ROBOCRANE is a blend of parallel mechanisms where the rigid links are replaced by cables, which is the basis of a CDPR (Albus et al., 1993). The robot has six cables, controlled with individual winches which are driven by servomotors (Bostelman, Albus, Dagalkis, Jacoff, & Gross, 1994). A year later, an ultrahigh-speed CDPR termed FALCON was developed in Japan, employed with PD controlled servomotors (Kawamura et al., 1995).

The first recorded application of CDPR was in 2003 as a material handler (United States of America Paten No. US6826452B1, 2003). It displayed the ability of CDPR to generate big workspace. This leads to the development of a method analysis named Specified Robustness Workspace (Bosscher P. M., 2004) and Wrench Feasible Workspace (Bosscher, Riechel, & Ebert-Uphoff, 2006). Control systems are also being developed, such as Lyapunov-based combined with feedback linearization PD controller (Alp and Agrawal, 2002) and quadratic programming combined with PD (Oh & Agrawal, 2005). Other supporting mechanisms in the CDPR also gained attention, with earliest work on reel friction modeling in Cable-Driven Locomotion (Otis, et al., 2009), followed by pulley mechanisms (Pott, 2012). The dynamic feasibility of the robot is also studied (Gosselin, 2012). This leads to the development of robust control, such as Lyapunov based PID which deals with cable uncertainty (Khosravi and Taghirad,

2014a) (Khosravi et al., 2013) and cable elasticity (Khosravi and Taghirad, 2014b). Sliding mode control (Hu et al., 2014). and system identification to model disturbance is also used in the development of a robust control system (Kraus et al., 2014). The vast development of the theoretical framework both in mechanical modeling and control system leads to several complex industrial applications such as aircraft maintenance (Nguyen and Gouttefarde, 2014a), shore wind turbine painting and sandblasting (Gagliardini et al., 2014), and large structures in general (Nguyen et al., 2014b).

One major drawback of CDPR is cable collision. This is addressed by using a combination of swept base and shortest distance algorithm (Blanchet and Merlet, 2014). The flexible nature of cables also introduces sag, which is started to be studied (Merlet J.-P. , 2015). Apart from that, the sagging nature can also affect its position accuracy (Jung et al., 2016), therefore force sensors are needed. Placing measurement sensors in pulleys are one of the examples (Kraus et al., 2015).

Within the past five years, the focus of research has started to shift to trajectory planning (Tempel et al., 2015) and reconfigurability of the CDPR (Gagliardini et al., 2016). Not only that, but the robot prospect in producing high-speed motion is also backed by the broad study in the dynamics of the parallel robots, such as Dynamic Feasible Workspace (DFW) (Gagliardini et al., 2017) (Baklouti et al., 2017). To enhance practicality, a simulation tool is also developed (Merlet J. P., 2017).

Pre - compensations are also added to the system such as grids to calculate distortion of the trajectory termed black box (Schmidt et al.,2017) is done to the system. Also, improvements on vibration are proposed by using active stabilizer (Lesellier et al., 2018), differential flatness (Yoon et al., 2018) or adding pre-compensations (Picard et al., 2018b) along with torque control (Picard et al., 2018a) (Begey et al., 2019) and cable elasticity (Baklouti et al., 2019). Also, the singularity of the CDPR concerning sagging cables is studied to identify unreachable workspace (Merlet J. P., 2019).

Research on CDPR to aid search and rescue operations has been established as early as the past decades to search for human bodies (Takemura, et al., 2004) (Bosscher et al., 2005). The objectives of the CDPR to aid search and rescue operations are being expanded by the team to substitute heavy machinery. Dimension synthesis (Nurahmi et al., 2017), design optimization (Hanafie et al., 2018), and static workspace analysis (Handojo, et al., 2018) for both fully constrained and suspended CDPR has been carried out as preliminary studies. The team also develops the mobile version of CDPR with the same purpose (Marvel, 2019).

2.2. Theoretical Background

The Theoretical Background of this research comprises of Cable-Driven Parallel Robot and Control Theory

2.2.1. Cable-Driven Parallel Robots

There are two types of CDPR based on the number of cables and its placement, namely fully constrained and suspended CDPR. Fully - constrained is suitable for high-speed operations since two cables are assigned for each DoFs to maintain tension, whereas suspended CDPR only has one. To move, suspended CDPR relies on the weight of the platform to maintain the tension. An example of a fully constrained planar 4-cable 3-DoF Cable-driven parallel robot is shown in Figure 2.3(a) and an example of a spatial 6-cable cable-suspended parallel mechanism is shown in Figure 2.3(b) (Gosselin, 2013).

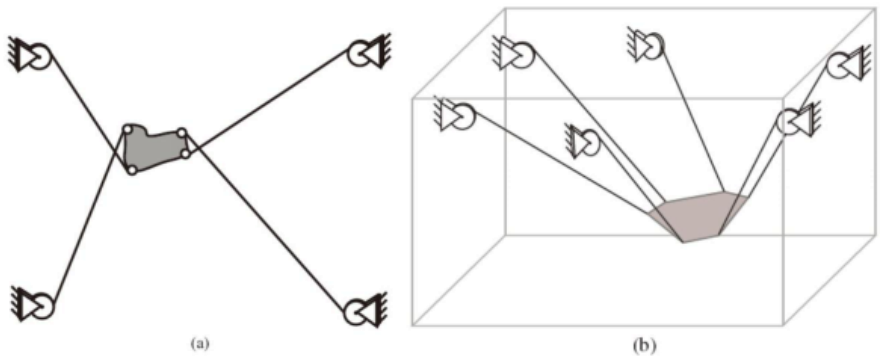

Figure 2.3. Cable-Driven Parallel Robot (a) Fully Constrained (b) Suspended (Gosselin, 2013)

2.2.1.1. Geometric Analysis

A Cable-Driven Parallel Robot with *m* cables is used as base for modeling the CDPR, as shown in Figure 2.4. The cables are parallel with respect to each other. The robot consists of a fixed frame, a moving platform, *m* sets of cables, pulleys and winches. The cables are attached to a moving platform at one end, and a winch on the other end. In between them, pulleys are attached to each top side of the fixed frame base. The cables run through the pulley on the top before resting onto the winches. These winches are actuated with motors, which are mounted on the bottom of the fixed frame base. The winches are used to control the moving platform by controlling the cable length on each respective point. The coiling and uncoiling of each winch will manipulate the cable length and therefore exerting tension to move the moving platform to the desired position. This research focuses on modeling a suspended CDPR with four cables (m = 4).

The fixed frame has a coordinate system denoted by F_b (x, y, z) and is placed on the bottom of the fixed frame, with length l_b, width w_b, and height h_b. The origin of the base frame is denoted by point O. F_b is the reference point. The moving platform has its local coordinate denoted by F_p (u, v, w) and is placed on the center of the moving platform with l_p, width w_p, and height h_p. The geometric center of the moving platform is denoted by point P and its position coordinate expressed in the base frame is denoted by ${}^{b}\mathbf{p} = [p_x \quad p_y \quad p_z]^T$. . Rotations about x, y, and z axes are denoted by ψ, θ, and ϕ. They are called the roll, pitch, and yaw

respectively. Combining the translational and rotational positions of the moving platform resulting in:

$$\boldsymbol{X} = [p_x \quad p_y \quad p_z \quad \psi \quad \theta \quad \phi]^T \tag{2.1}$$

The pulley is attached to each side on the top of the fixed frame, referred to as exit points A_i, where $i = 1 \ldots m$. The position vector of these exit points is expressed with respect to the base frame F_b, denoted as ${}^b\mathbf{a}_i = [a_x \quad a_y \quad a_z]^T$. Each side of the moving platform attached to the cables is referred to as anchor points B_i, where $i = 1 \ldots m$. The position vector of these anchor points is expressed with respect to the platform frame F_p, denoted as ${}^p\mathbf{b}_i = [b_x \quad b_y \quad b_z]^T$.

To express the moving platform coordinates F_p relative to the base frame O, rotation matrix R is introduced and expressed as follows:

$$R(\psi, \theta, \phi) = R_z(\psi) R_y(\theta) R_x(\phi)$$
$$= \begin{bmatrix} c(\psi)c(\theta) & c(\psi)s(\theta)c(\phi) - s(\psi)c(\phi) & c(\psi)s(\theta)c(\phi) + s(\psi)c(\phi) \\ s(\psi)c(\theta) & s(\psi)s(\theta)s(\phi) - c(\psi)c(\phi) & s(\psi)s(\theta)s(\phi) + c(\psi)c(\phi) \\ -s(\theta) & c(\theta)s(\phi) & c(\theta)c(\phi) \end{bmatrix} \tag{2.2}$$

This represents the orientation of the moving frame with respect to the base frame. The cable vector is denoted as ${}^b\mathbf{l}_i$, where $i = 1 \ldots m$. Therefore, by using loop closure, the vector of cable lengths can be determined as follows:

$${}^b\mathbf{l}_i = {}^b\mathbf{a}_i - {}^b\mathbf{p} - \mathbf{R}\, {}^p\mathbf{b}_i \tag{2.3}$$

The unit vector of cables is derived as:

$${}^b\hat{\mathbf{l}}_i = \frac{{}^b\mathbf{l}_i}{\| {}^b\mathbf{l}_i \|} \tag{2.4}$$

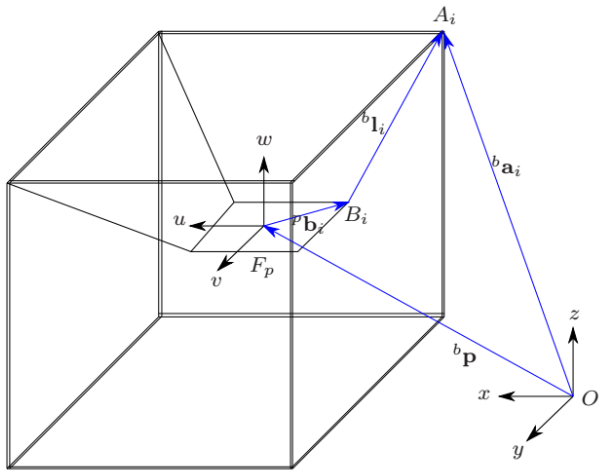

Figure 2.4. Geometric Modelling of Cable-Driven Parallel Robot

2.2.1.2. Kinematic Analysis

The kinematic model of CDPR is an analysis to obtain the input-output relationship between the cable velocity and the moving platform velocity, with no regard for the forces that causes the motion. Since controlling cable length will also control the moving platform, knowledge of cable velocities is important. Those cables act as actuators which are driven by a motor having a certain limit of velocity and acceleration.

The relationship between the moving platform velocity ad cable velocities is defined as:

$$\mathbf{Jt} = \dot{\mathbf{l}} \tag{2.5}$$

where **J** is the Jacobian matrix, **t** is the moving platform velocity or twist, and $\dot{\mathbf{l}}$ is cable velocities. Jacobian matrix is used to transform the moving platform velocity to cable velocity. It is expressed as:

$$\mathbf{J} = \mathbf{W}^T \tag{2.6}$$

The twist of the moving platform is expressed as:

$$\mathbf{t} = [\dot{p}_x \quad \dot{p}_y \quad \dot{p}_z \quad \dot{\phi} \quad \dot{\theta} \quad \dot{\psi}]^T \tag{2.7}$$

Where the cable velocity of the CDPR is expressed as:

$$\dot{\mathbf{l}} = [\dot{l}_1 \quad \dot{l}_2 \quad \dot{l}_3 \quad \dot{l}_4] \tag{2.8}$$

2.2.1.3. The dynamic model of the CDPR

The dynamic model of the CDPR is an analysis carried out with a certain amount of forces and moments are imposed onto the moving platform. The dynamic equilibrium equation for the system is expressed as follows:

$$\mathbf{W}\tau + \mathbf{w}_e = m\mathbf{a} \tag{2.9}$$

W is a wrench matrix, consists of forces and moments unit vectors exerted by *m* cables to the platform, which can be mathematically expressed as follows:

$$\mathbf{W} = \begin{bmatrix} \hat{\mathbf{l}}_1 & \hat{\mathbf{l}}_2 & \hat{\mathbf{l}}_3 & \hat{\mathbf{l}}_4 \\ \mathbf{R}\,{}^p\mathbf{b}_1 \times \hat{\mathbf{l}}_1 & \mathbf{R}\,{}^p\mathbf{b}_2 \times \hat{\mathbf{l}}_2 & \mathbf{R}\,{}^p\mathbf{b}_3 \times \hat{\mathbf{l}}_3 & \mathbf{R}\,{}^p\mathbf{b}_4 \times \hat{\mathbf{l}}_4 \end{bmatrix} \tag{2.10}$$

τ is a vector consisting of m cable tensions, which is defined as $\boldsymbol{\tau} = [\boldsymbol{\tau}_1 \quad \boldsymbol{\tau}_2 \quad \boldsymbol{\tau}_3 \quad \boldsymbol{\tau}_4]$. $\mathrm{w_e}$ is an external wrench applied to the platform. It consists of external forces and moments as follows:

$$\mathbf{w}_\mathrm{e} = [\mathrm{f} \quad \mathrm{m}]^T = [f_x \quad f_y \quad f_z \quad m_x \quad m_y \quad m_z]^T \tag{2.11}$$

The components of the external wrench are constrained within the given boundary as follows:

$$f_{min} \leq f_x, f_y, f_z \leq f_{max} \tag{2.12}$$
$$m_{min} \leq m_x, m_y, m_z \leq m_{max}$$

Let the gravitational acceleration is $g = 9.8\ {}^{m}/_{s^2}$. The component of the external wrench considered in this research is only the weight of the platform. Therefore, the external wrench $\mathbf{w}_\mathrm{e}$ can be defined as:

$$\mathbf{w}_\mathrm{e} = [0 \quad 0 \quad m\mathbf{g} \quad 0 \quad 0 \quad 0]^T \tag{2.13}$$

The acceleration of the moving platform determined upon the derivation of Equation 2.9 becomes:

$$\mathbf{a} = [\ddot{p}_x \quad \ddot{p}_y \quad \ddot{p}_z \quad \ddot{\phi} \quad \ddot{\theta} \quad \ddot{\psi}\ ]^T \tag{2.14}$$

Rearranging Equation 2.9 to compute cable tension τ becomes:

$$\mathbf{W}\tau = m\mathbf{a} - \mathbf{w}_e \tag{2.15}$$

Substitution of Equation 2.13 and Equation 2.14 to Equation 2.15 along with simplification gives:

$$\mathbf{W}\tau = m\mathbf{a} - m\mathbf{g} \tag{2.16}$$

Finally, the cable tension can be solved as:

$$\tau = \mathbf{W}^{\dagger} m(\mathbf{a} - \mathbf{g}) \tag{2.17}$$

The wrench matrix is a 6 – by – 4 matrix, which makes W to be a non-symmetric matrix. Hence, the system is classified as an underdetermined problem. If the tension values are substituted back into Equation 2.17, this equation will not vanish but instead, an error introduced as ε:

$$\varepsilon = \mathbf{W}\tau + m(\mathbf{g} - \mathbf{a}) \tag{2.18}$$

2.3. Stepper Motor

Stepper motor is a motor in which the rotor can generate discrete stationary angular positions. The main characteristic of using stepper motor is that it can be operated as an open-loop system, exhibits high torque at a small angular velocity which is useful in accelerating the payload up to speed. The main advantage of having a stepper motor as an actuator is that the error is non-cumulative which makes it an excellent position controller. It also does not need an encoder as a measurement sensor, cutting set up cost.

The response of a stepper motor has an underdamped property when moving from one step to another. This is shown when the phase is changed to the adjacent stator teeth combination, moving the rotor to the new equilibrium point. In reaching the equilibrium point, the torque is zero whereas the angular velocity of the rotor is not zero. Therefore, overshoot occurs in the equilibrium position. The rotor generated torque to compensate for the position back to the equilibrium point. This phenomenon occurs a few times until the rotor comes to rest. In general, the magnitude and duration of the damped oscillation are dependent on the step angle. The larger the angle, the larger overshoot it produces (Klafter, Chmielewski, & Negin, 1989).

2.4. CDPR Control System

In this section, three control systems are described, which will be served as references in developing the control system.

2.4.1. Design and Control of Suspended Cable-Driven Parallel Robot with Four Cables (Mersi et al., 2018)

A. Research Objective

A design and position control problem of a suspended 4 – cables - driven parallel robot is addressed by a team from Iran. The usual design with winches as means of coil – uncoil the cables leads to a major error in estimating the cable length. To enhance cable lengths estimation, a roller screw is employed to ensure that the cables coil one layer each. The research focuses on developing a way to generate pose in real-time by employing an angular rate sensor in the end effector. The data obtained from the sensor is used to estimate the position of the end effector by using forward geometric. Since solving forward geometric problem in parallel manipulators is harder than its inverse, a new method of solution is also proposed.

B. Proposed System

The team builds a suspended cable-driven parallel robot with four cables as shown in Figure 2.5 (a). The exit points of the robot are mounted on the ceiling, along with the winches and the motors. An encoder is placed within the motor to derive the cable length with additional data of the cable's initial length. The end effector is a rectangular platform in which a Magnetic Pickup Unit (MPU) sensor is placed. Due to the nature of cables that can only be pulled, only three DOFs (x, y, z) out of six can be controlled. Also, the team assumed the end effector as a point of mass, on basis that the size is negligible in contrast to the robot dimension. With this assumption, the orientation of the end effector becomes constant, and the end effector position can directly be used to solve the forward kinematics problem.

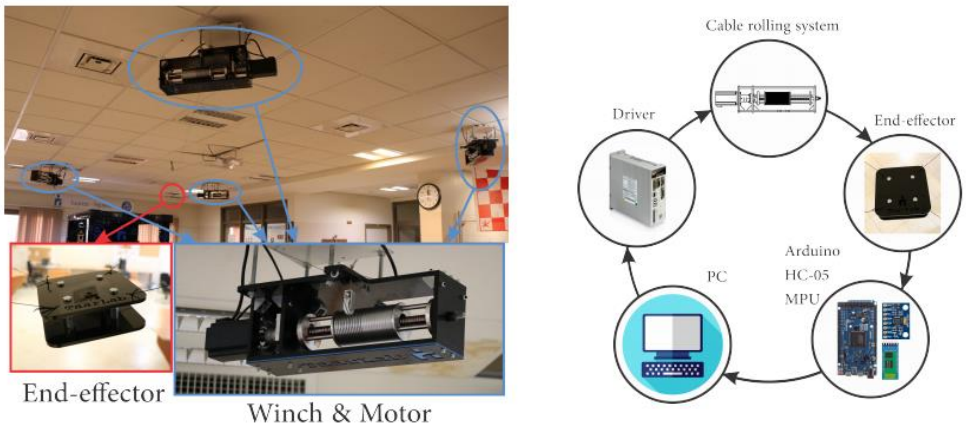

(a) (b)

Figure 2.5. (a) Prototype (b) General View of Experimental Setup (Mersi et al., 2018)

The general view of the control system is shown in Figure 2.5(b). The MPU sensor used is a 9-DOF Inertial Measurement Unit containing a gyroscope, accelerometer, and magnetometer, each has three axes. The data combinations of these three sensors will result in roll, pitch, and yaw angles of the end effector with minimal error. The angles will then be used as an input to estimate the position of the end effector using forward kinematics, which will be compared to the desired position to compute the error. The error is mapped into the joint space using the Jacobian matrix and will be compensated by the controller using PID, with gains obtained from trial and error. The controller will adjust the speed of the motor, proportional to the error.

2.4.2. Robust PID Control of Fully - Constrained Cable-Driven Parallel Robots (Khosravi and Taghirad, 2014a)

A. Research Objectives

The goal is to develop a theoretical framework for robust position control of CDPR based on a simple PID Controller structure. Within the development of the theoretical framework, uncertainties are also modeled while considering its robustness on the stability of the closed-loop system by including the proposed algorithm. A corrective term is also introduced, interpreted as internal forces, obtained based on the null space of the transposed Jacobian matrix of the robot. The

proposed scheme is then applied to a four-cables-driven parallel robot to show the effectiveness of the proposed algorithm, as shown in Figure 2.6.

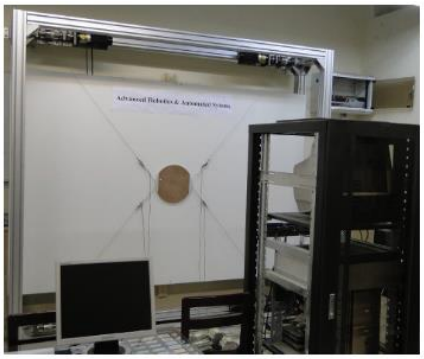

Figure 2.6. CDPR prototype (Khosravi and Taghirad, 2014a)

B. Proposed Method

Several assumptions are made throughout the paper, which are:

1. The motion is within the wrench closure workspace
2. Nonlinear dynamic equations of the cable robot are uncertain with only partial knowledge is known.

The control system setup is shown in Figure 2.7 (a). The proposed control strategy employs a cascade control system with two loops. The outer loop is designated for position control and consists of the proposed PID controller, with gains obtained through the experiment. Inputs of this loop are the desired position and orientation, and the output is the required cable tension. The inner loop is designated to compare the desired tension with the actual tension and try to minimize the error by using a lag controller. The actual tension is measured using load cells located near the end effector attachment points. The cable lengths will then be fed to a forward kinematic equation to estimate the position of the end effector.

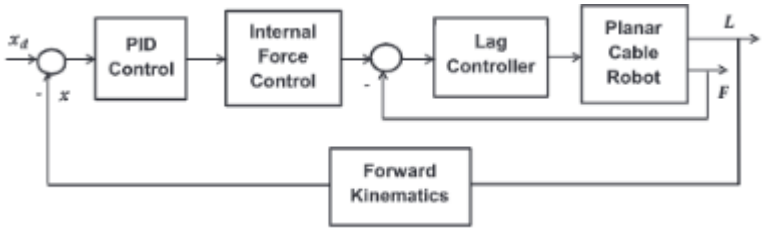

(a)

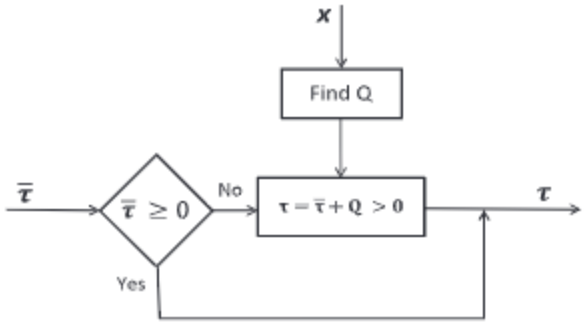

(b)

Figure 2.7. (a) Proposed Scheme (b) Internal Force Control (Khosravi and Taghirad, 2014a)

The results are shown in Figure 2.8 (a) and (b). When the controller is introduced with uncertainties such as payload and disturbance, it can stabilize the system while producing positive tension, as shown in Figure 2.8. (a). Also, the proposed control scheme is tested under a circular trajectory, with the result shown in Figure 2.9 (b).

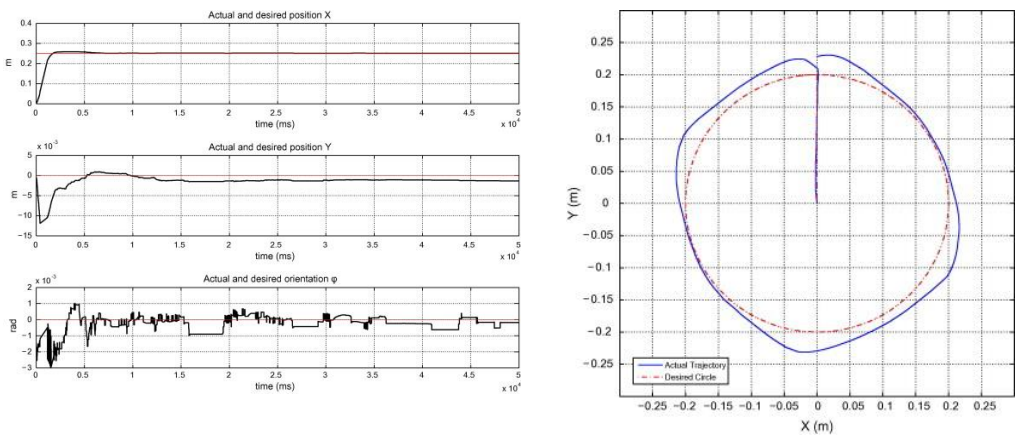

Figure 2.8. (a) Error Tracking with respect to Uncertainties (b) Circular Trajectory Generation within the End Effector (Khosravi & Taghirad, 2014)

CHAPTER 3

RESEARCH METHODOLOGY

3.1. General Flowchart

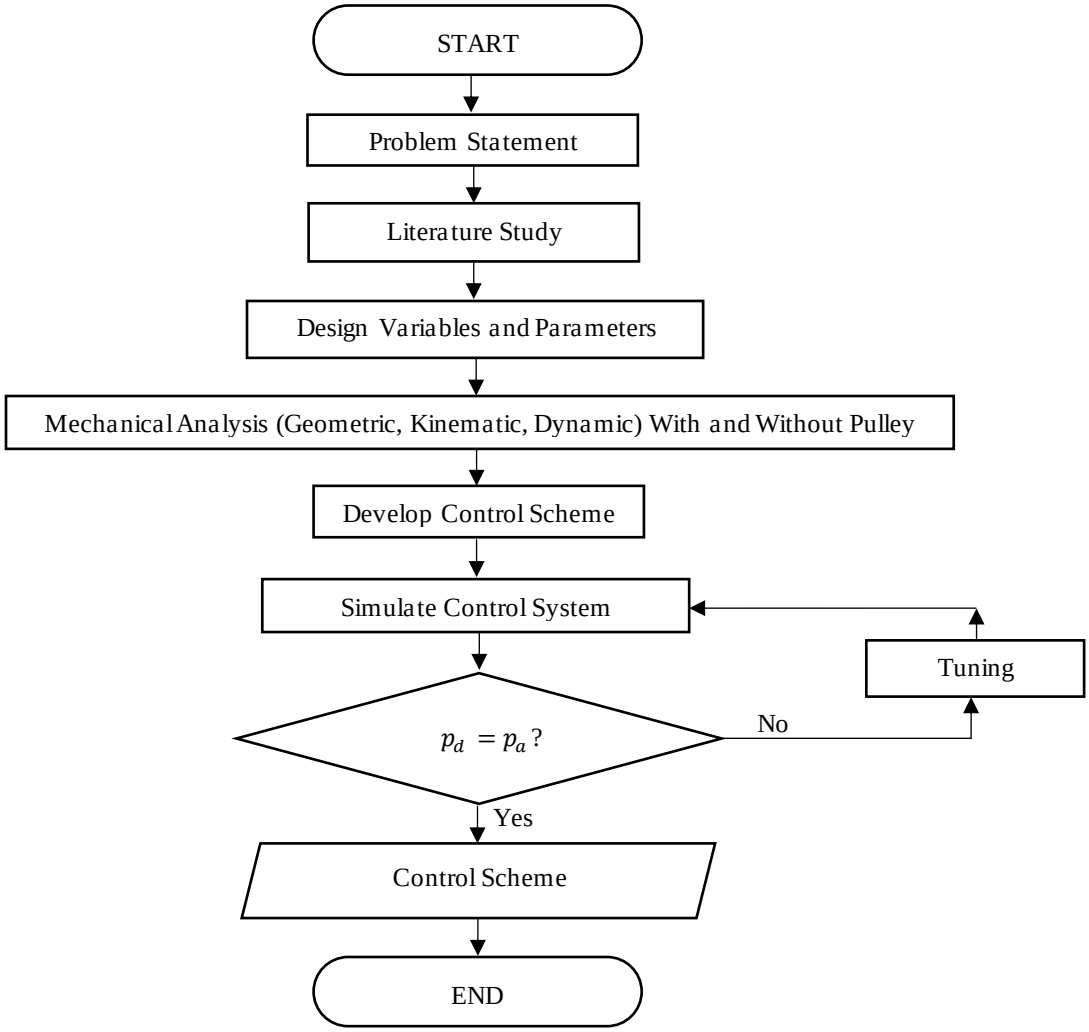

Figure 3.1. General Research Flowchart

3.1.1. Mechanical Flowchart

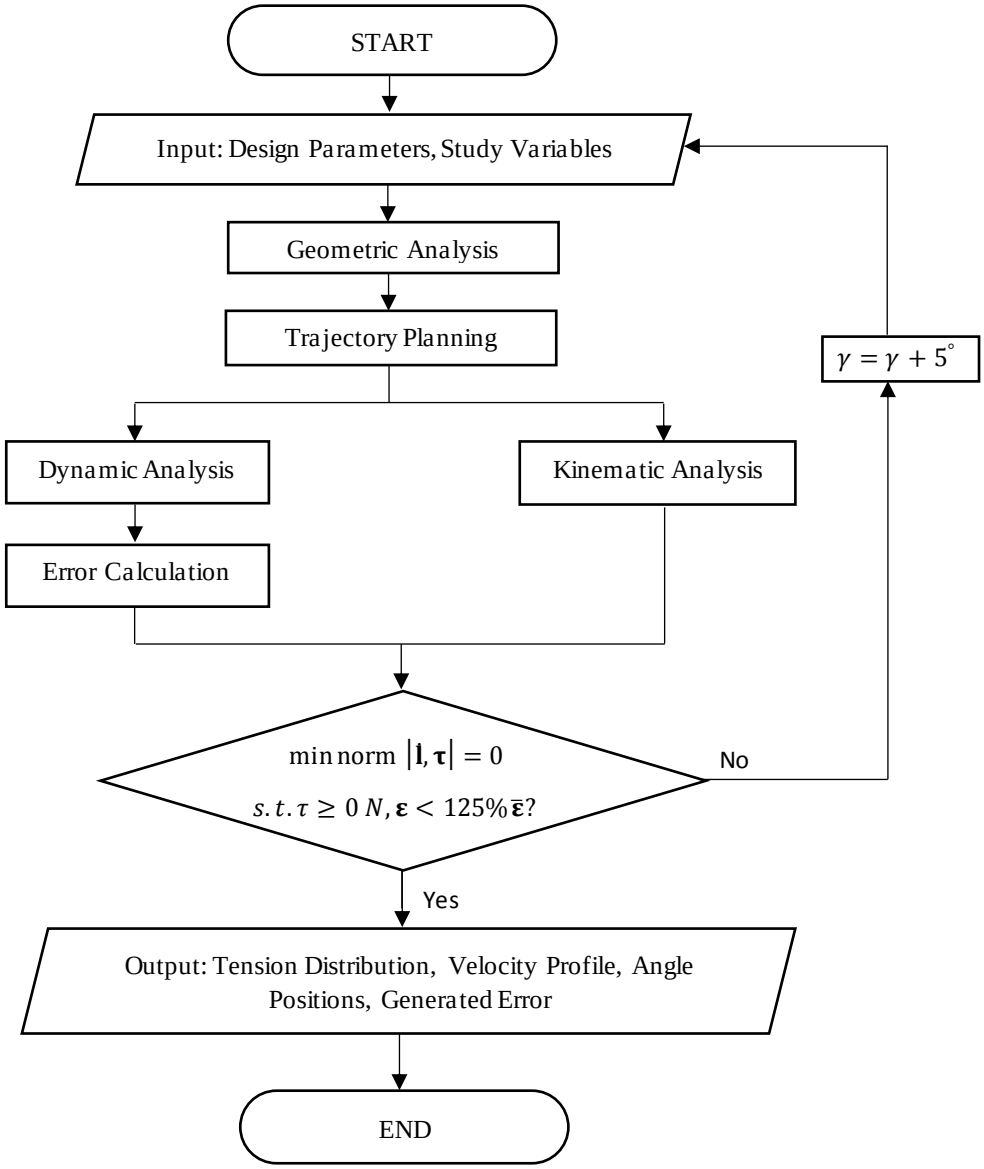

Figure 3.2. Mechanical Flowchart

3.1.2. Control Scheme Flowchart

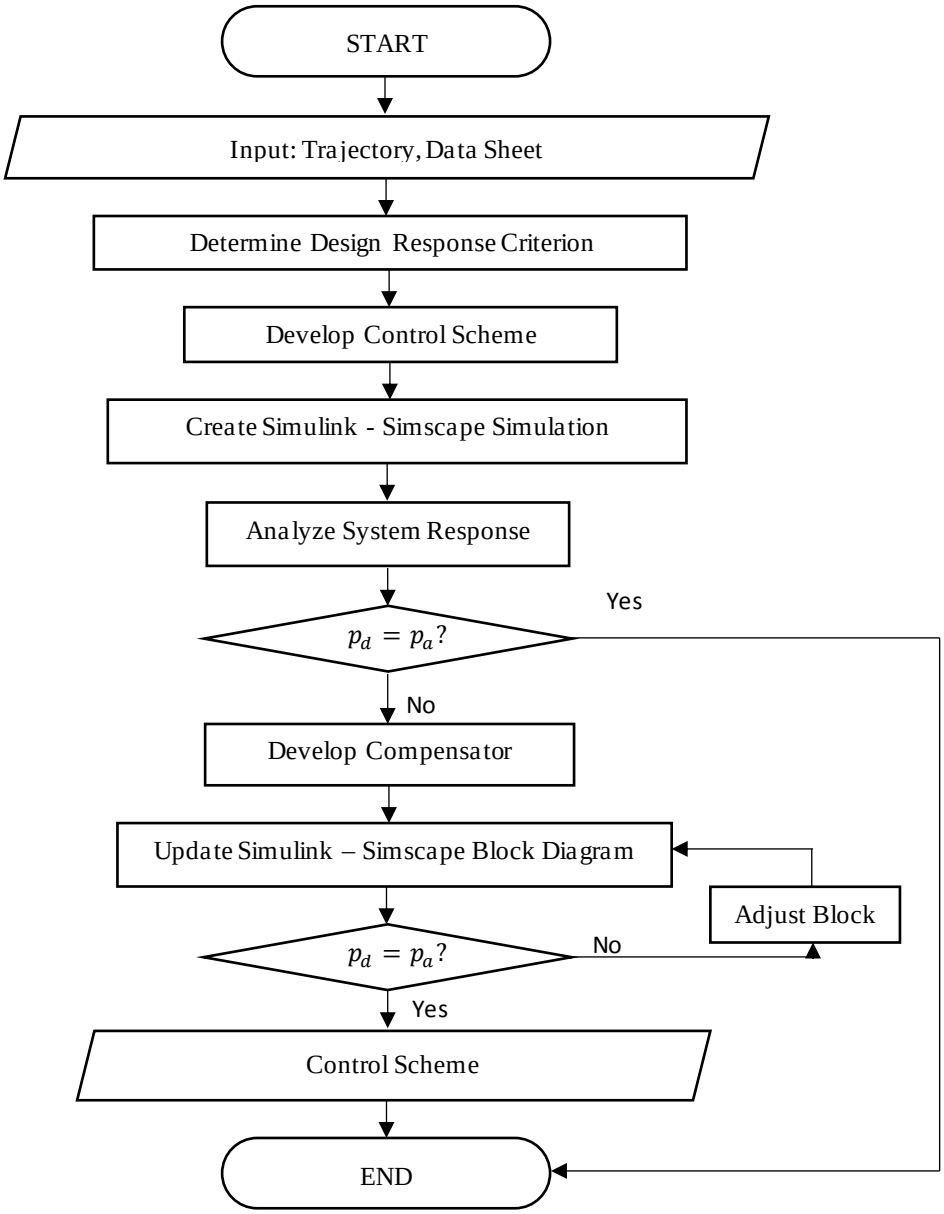

Figure 3.3. Control Scheme Flowchart

3.2. Research Process

3.2.1. General Flowchart

1. Problem Statement

Data collection and analysis are carried out on natural disasters in Indonesia. From these data, problems can be justified and served as a base for the literature study.

2. Literature Study

A literature study is carried out to gather insights regarding past works and the basic theory of the defined problem. It is done by reading written works such as books, journals, and past research.

3. Design Parameters and Variables in the Study

Mechanical design parameters such as the number of cables, dimensions of the fixed frame, dimensions of the moving platform are determined. Furthermore, several trajectories and reconfigurable parameters such as end effector trajectories and increments used on reconfigurable pulleys are determined. In this research, sinusoidal motion, circular and vertical helix are used as the simulated trajectories. In terms of the control system, the outputs from the mechanical analysis will be used as control parameters, which in turn will give the required control scheme.

4. Mechanical Analysis (Geometric, Kinematic, Dynamic) With and Without Pulley

The geometric model of the CDPR with the influence of pulleys is derived, which considers the stated design parameters. Also, kinematic, and dynamic analyses are carried out. The aims are to find the tension distribution, velocity profile, and the angles. By considering the pulley mechanism, the robot will be able to reconfigure and fulfill the positive tension requirements while retaining the smallest error and cable velocity.

5. Develop Control Scheme

The resulting tension distribution, along with its velocity profile and pulley angles are taken as input reference for controlling the CDPR. In this step, the block diagram for the overall scheme, along with its subsystem is developed.

6. Simulate Control Scheme

To achieve the requirements, the system will be compensated using PI/PD/PID Control. The gain will be used as a reference to control the prototype.

7. Expected Output

The expected output of this study is the actual working prototype of the CDPR which meets the desired design requirements of the system.

3.2.2. Influence of Pulley Flowchart

1. Design Parameters and Variables in the Study

Design parameters such as the number of cables, dimensions of the fixed frame, dimensions of the moving platform are determined with reference to past works, and the constructed prototype. Furthermore, several parameters such as end effector trajectories and increments used on reconfigurable pulleys are pre-determined. Also, parameters regarding the planned trajectories such as initial height z_0, oscillation frequency ω, the initial position of the moving platform, and radius of motion r has been decided beforehand. In this research, sinusoidal motion, circular and vertical helix are used as the simulated trajectories.

2. Geometric Analysis

The geometric of the cable is analyzed by using the loop closure equation, with cable length is mathematically expressed as:

$$ {}^{b}\mathbf{l}_i = {}^{b}\mathbf{c}_i - {}^{b}\mathbf{p} - \mathbf{R}\,{}^{b}\mathbf{b}_i, i = 1, \dots, 4 \tag{3.1} $$

Where ${}^{b}\mathbf{l}_i$ is cable length vector from exit point i to anchor point i, ${}^{b}\mathbf{c}_i$ is the vector of pulley *contact points* with respect to the base frame, ${}^{b}\mathbf{p}$ the position

vector of the moving platform with respect to the base frame, **R** is thenrotation matrix and ${}^{p}\mathbf{b}_i$ vector of anchor points with respect to the moving platform.

3. Trajectory Planning

The trajectories discussed in this research are referred to as the works of Gosselin (Gosselin, 2012). The lists range from sinusoidal motion, which is the simplest, to more complex ones such as the vertical helix.

A. Sinusoidal Motion

To demonstrate the ability of the model to follow a dynamic path, the simplest form of trajectory is studied. A sinusoidal motion passing through the base of the frame through the Z-axis is modeled as:

$$p_x = p_y = 0, p_z = z_0 + rsin(\omega t) \quad z_0 > r \tag{3.2}$$

Where p_x, p_y, p_z are the positions of the pose with respect to the base frame. ω is the oscillation frequency, z_0 is the initial height of the platform and r is the amplitude of the oscillation. Derivating the equation with respect to time gives:

$$\dot{p}_x = \dot{p}_y = 0, \dot{p}_z = r\omega cos(\omega t) \tag{3.3}$$

Where $\dot{p}_x, \dot{p}_y, \dot{p}_z$ are the velocity of the pose with respect to the base frame. Derivating the equation with respect to time to compute acceleration:

$$\ddot{p}_x = \ddot{p}_y = 0, \ddot{p}_z = -r\omega^2 sin(\omega t) \tag{3.4}$$

B. Circular Trajectory

The second motion to be studied is the circular trajectory. Let us consider a circle situated at $(0,0,z_0)$ rotating with respect to the Z-axis. The pose based on the trajectory can be stated as:

$$p_x = rcos(\omega t), p_y = rsin(\omega t), p_z = z_0 \tag{3.5}$$

Where p_x, p_y, p_z are the positions of the pose in with respect to the base frame. ω is the oscillation frequency, z_0 is the initial height of the platform. The velocity of the moving platform can be determined by derivating the equation with respect to time, which gives:

$$\dot{p}_x = -r\omega sin(\omega t), \dot{p}_y = r\omega cos(\omega t), \dot{p}_z = 0 \tag{3.6}$$

Where $\dot{p}_x, \dot{p}_y, \dot{p}_z$ are the velocity of the pose with respect to the base frame. The acceleration of the moving platform can be found by derivating the equation with respect to time, which resulted in:

$$\ddot{p}_x = -r\omega^2 cos(\omega t), \ddot{p}_y = -r\omega^2 sin(\omega t), \ddot{p}_z = 0 \tag{3.7}$$

C. Vertical Helix

To demonstrate the ability of the CDPR along a more complex trajectory, a vertical helix is constructed. A circular trajectory rotating with respect to the Z-axis is modeled as:

$$p_x = rcos(\omega_1 t), \quad p_y = rsin(\omega_1 t), \quad p_z = z_0 + hsin(\omega_2 t), \quad z_0 > r \tag{3.8}$$

Where p_x, p_y, p_z are the positions of the pose in with respect to the base frame. ω_1 is the frequency of the rotating motion and ω_2 is the frequency of the vertical oscillation. z_0 is the initial height of the platform. The velocity of the moving platform can be determined by derivating the equation with respect to time, which gives:

$$\dot{p}_x = -r\omega_1 sin(\omega_1 t), \quad \dot{p}_y = r\omega_1 cos(\omega_1 t), \quad \dot{p}_z = h\omega_2 cos(\omega_2 t) \tag{3.9}$$

Where $\dot{p}_x, \dot{p}_y, \dot{p}_z$ are the velocity of the pose with respect to the base frame. The acceleration of the moving platform can be found by derivating the equation with respect to time, which resulted in:

$$\ddot{p}_x = -r{\omega_1}^2 cos(\omega_1 t), \quad \ddot{p}_y = -r{\omega_1}^2 sin(\omega_1 t), \quad \ddot{p}_z = -h{\omega_2}^2 cos(\omega_2 t) \tag{3.10}$$

4. Dynamic analysis of the CDPR

Dynamic analysis of the CDPR is carried out based on Newton's second law of motion. The dynamic analysis considers forces and moments applied to the mechanism.

$$\mathbf{W}\tau + \boldsymbol{w_e} = m\ddot{\mathbf{p}} \tag{3.11}$$

Where $\mathbf{W}$ is the wrench matrix, τ is cable tension, $\boldsymbol{w_e}$ is the external wrench, m is the payload mass and $\ddot{\mathbf{p}}$ is the acceleration vector of the moving platform.

5. Error calculation

Next is to determine the calculation error generated from the calculation. The error can be calculated as:

$$\varepsilon = \mathbf{W}_\tau + m(\mathbf{g} - \ddot{\mathbf{p}}) \tag{3.12}$$

Where ε is the generated error and $\mathbf{g}$ is the gravitational acceleration.

6. Kinematic analysis of the CDPR

The kinematic behavior of the CDPR is studied, to obtain an input-output relationship between cable velocity and the moving platform, without looking at the forces causing the motion. This relationship can be defined as:

$$\mathbf{Jt} = \dot{\mathbf{l}} \tag{3.13}$$

Where $\mathbf{J}$ is the Jacobian matrix of the system, $\mathbf{t}$ is platform twists and $\dot{\mathbf{l}}$ is cable velocities.

7. Comparison to the desired values

Tension distributions for each cable are determined based on the norm minimization problem of both the cable velocity and error produced. If the desired values are not met, then the pulley will reconfigure until it matches the stated requirements.

8. The output from Dynamic, Kinematic, Geometric Analysis

From the analysis, tension distribution, angle positions, generated error, and velocity profile are obtained and observed.

3.2.3. Control Scheme Flowchart

1. Input Variables

Desired trajectory and motor datasheet are used to develop the control scheme. The desired trajectory is used to generate the set point of the stepper motor, and the motor data sheet is used as supporting data to construct simulation in Simulink – Simscape environment.

2. Determine the design response criterion

Position error is used as the design criterion. The control scheme is developed with this requirement in thought.

3. Develop Control scheme

The control scheme is developed in reference to past works as stated in the literature review. The position is the controlled variable. Through several calculations, this value is translated into the desired number of steps for each motor. The result is a block diagram that can be simulated through Simulink – simscape environment.

4. Create Simulink – Simscape simulation

The Block diagram is constructed in Matlab. Simulink is used to calculate the reference point (converts position into number of steps), while Simscape is used to simulate the physical behavior of the stepper motor.

5. Analyze System Response

Response plots are obtained through each simulation. These plots are analyzed. If the requirement is met, then the block diagram will be embedded in the system. If not, a compensator will be added.

6. Develop Compensator

The compensator is developed to improve the design requirement of the system. The error compensation scheme is added to reduce the position error of the system.

7. Update Simulink – Simscape Block Diagram

The proposed compensator(s) is/are added to the existing Simulink – simscape. The updated control scheme is then simulated to see whether the compensator(s) can give the desired response. If yes, then the block diagram will be embedded in the system. If not, then the parameters are adjusted until errors are acceptable.

8. Expected Output

Outputs such as block diagram, along with the values of compensator(s) will be the expected output of the system.

CHAPTER 4

RESULT AND DISCUSSION

The main objective of this research is to develop a cable robot for search – and – rescue operations. The cable robot must have several design requirements as follows:

1. Big workspace and high payload
2. Always able to fulfill the required trajectory.
3. Can be easily assembled and disassembled

Point one has already been studied. First, dimension synthesis has been analyzed for fully constrained suspended cable robot (Nurahmi, et al., 2017), Second, optimum cable arrangement for four cables suspended cable robot (Hanafie et al., 2018). Third, interference-free workspace of the suspended cable robot (Handojo, et al., 2018). The main goal of this thesis is to simulate the behavior of the robot under a dynamic trajectory and develop a control scheme to be implemented into a prototype.

The robot is designed to pick up large debris (e.g. ruins). The heavy load needs to be lifted by the cables while performing a determined trajectory, such as moving from left to right. Upon this movement, dynamic effects are present in the system. To ensure that the robot can move in the determined trajectory while carrying the load, the trajectory needs to be in the robot's dynamic workspace. The dynamic workspace encompasses trajectory points where the intended accelerations of the robot can be generated while in between the upper and lower tension limits (Gagliardini et al., 2017). It is noteworthy that cables can only be pulled, but not pushed. This implies that tension on each cable should be positive. Therefore, lower tension limits should be greater than zero. The upper tension limits should correlate with the maximum generated torque of the actuators.

In certain cases, the planned trajectory can be out of the robot's dynamic workspace. This leads to tension not in its limits. One approach to address this issue is by introducing reconfigurability to CDPR. Reconfigurability is important due to its ability to adapt within the work environments of the cable robots. Most of the reconfigurable CDPRs are on its exit point (Nguyen and Gouttefarde, 2014a) (Gagliardini et al.,, 2014), and anchor points (Barbazza et al., 2017). Apart from adaptability, the advantage of having Reconfigurable CDPRs is the extension of the feasible workspace. Intuitively, changing the exit or anchor points will change the wrenches, which in turn changes the tension. Consequently, manipulating these points through reconfigurability enables the expansion of its dynamic workspace.

For search and rescue operations, this might prove to be impractical. The reason is that reconfiguring either the exit points or the anchor points on the actual robot requires prismatic joints as means of actuation, which need to be controlled and equipped with sensors to gather the actual position. This does not meet one of the important design requirements of the search and rescue CDPR, which is the ability to be assembled and disassembled with speed. To address this issue, we propose a reconfigurable pulley that can be set at certain angles. Controlling angles are much simpler since it can be actuated by stepper motors which do not require sensors. Incorporating pulleys, the system changes the geometric analysis by introducing a new point termed contact point to the loop closure.

4.1. Mechanical Modelling of Suspended CDPR

Considering pulley kinematics changes the loop closure on cable lengths, from the exit points to the contact points situated at the point when the cables leave the pulleys. Three models are obtained from this mechanical modeling, namely geometric, kinematic, and dynamic equations. The geometric model is used to calculate cable length with respect to the pose position. The kinematic model is used to calculate cable velocities with respect to the pose velocity. Lastly, the Dynamic model is used to calculate cable tension with respect to pose acceleration and payload.

The analysis conducted in this section on the influence of pulleys to the dynamic trajectory of the robot has been published in International Journal on Dynamic and Control under paper title Dynamic Trajectory Planning of Reconfigurable Suspended Cable Robot (Syamlan et al., 2020). The study of dynamic trajectory itself has been published as a conference paper on the International Conference on Mechanical Engineering under the title Dynamic Trajectory Generation of Suspended Cable-Driven Parallel Robot (Syamlan et al., 2019).

4.1.1. Influence of Pulley Mechanism Derivation

A Cable-Driven Parallel Robot with four cables is used to model the dynamics of the CDPR, as shown in Figure 4.1. The influence of pulleys is considered in the derivation of the geometric model. Consider a pulley mechanism at exit point A_i as shown in Figure 4.2.(a) and Figure 4.2(b). This pulley has its local frame denoted as $F_{ai}(x_{ai}, y_{ai}, z_{ai})$, where $i = 1 \ldots 4$. Apart from exit point Ai, a contact point C_i, where $i = 1 \ldots 4$ is present at the opposite side of exit point A_i. These two points produce an angle, denoted as β_i. Also, the pulley has a center point, denoted as M_i, where $i = 1 \ldots 4$. It is situated at ${}^{a}\mathbf{m}_i = [m_x \quad m_y \quad m_z]^T$. The position vector of exit point A_i is denoted as ${}^{b}\mathbf{a}_i = [a_x \quad a_y \quad a_z]^T$, whereas the position vector of the contact point C_i is denoted as ${}^{b}\mathbf{c}_i = [c_x \quad c_y \quad c_z]^T$. If this pulley is to be looked from the top, the angle produced by the pulley from the x_i axis to the y_i axis is denoted as γ_i.

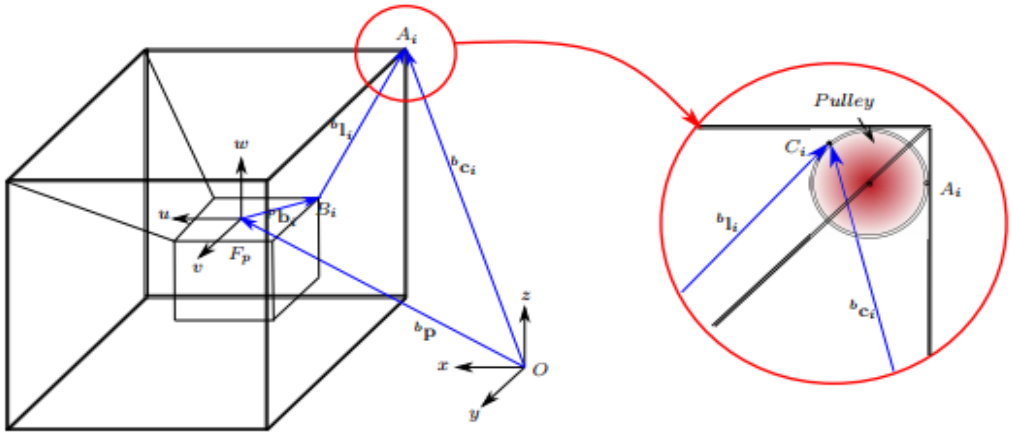

Figure 4.1. Geometric model of CDPR

The exit point A_i at the base frame acted as the first point, whereas contact point C_i as the last point of contact between the cable and the pulley, as shown in Figure 4.3(a). Therefore, by using loop closure, the vector of cable lengths can be determined as follows:

$$ {}^{b}\mathbf{l}_i = {}^{b}\mathbf{c}_i - {}^{b}\mathbf{p} - \mathbf{R}\,{}^{b}\mathbf{b}_i, i = 1, \dots, 4 \tag{4.1} $$

With its unit vector derived as:

$$ {}^{b}\hat{\mathbf{l}}_i = \frac{{}^{b}\mathbf{l}_i}{\| {}^{b}\mathbf{l}_i \|} \tag{4.2} $$

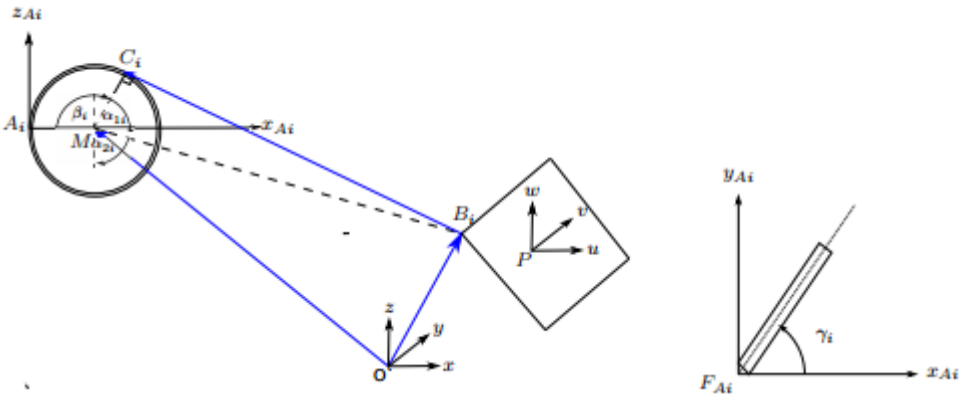

Figure 4.2. (a) Geometric model of Pulley (b) Top view

Notice that the influence of pulley has changed the loop closure in the geometric model of the CDPR. To find point C_i, the geometry model of the pulley mechanism is inspected, which can be derived as follows:

$$ {}^{b}\mathbf{c} = {}^{b}\mathbf{a} + {}^{a}\mathbf{am} + {}^{a}\mathbf{mc} \tag{4.3} $$

Where ${}^{b}\mathbf{c}$ is the position vector of the point C_i, ${}^{b}\mathbf{a}$ is the position vector of the point A_i, ${}^{a}\mathbf{am}$ is the position vector of the pulley center which is denoted as $[r \quad 0 \quad 0]^T$ and is equal to ${}^{a}\mathbf{mc}$. Vectors ${}^{a}\mathbf{am}$ and ${}^{a}\mathbf{mc}$ are still relative to the

pulley local frame F_{ai}. Both vectors have to be translated into the reference frame F_b. Therefore, rotation matrices $\mathbf{R}_z$ and $\mathbf{R}_y$ are introduced to transform these vector with respect to base frame coordinates F_b. The rotation matrices R_z and R_y are expressed as:

$$\mathbf{R}_z(\gamma) = \begin{bmatrix} c(\gamma) & -s(\gamma) & 0 \\ s(\gamma) & c(\gamma) & 0 \\ 0 & 0 & 1 \end{bmatrix} \tag{4.4}$$

$$\mathbf{R}_y(180-\alpha) = \begin{bmatrix} c(180^\circ-\alpha) & 0 & s(180^\circ-\alpha) \\ 0 & 1 & 0 \\ -s(180^\circ-\alpha) & 0 & c(180^\circ-\alpha) \end{bmatrix} \tag{4.5}$$

Substituting $\mathbf{R}_z$ and $\mathbf{R}_y$ into Equation 4.8. yields:

$$^b\mathbf{c} = \begin{bmatrix} a_x \\ a_y \\ a_z \end{bmatrix} + \mathbf{R}_z(\gamma)\begin{bmatrix} r \\ 0 \\ 0 \end{bmatrix} + \mathbf{R}_z(\gamma)\mathbf{R}_y(180-\alpha)\begin{bmatrix} r \\ 0 \\ 0 \end{bmatrix} \tag{4.6}$$

To find α , consider position vector of point M_i which can be written as:

$$^b\mathbf{om} + {}^p\mathbf{mb} = {}^b\mathbf{b} \tag{4.7}$$

Rearranging Equation 4.7 gives:

$$^p\mathbf{mb} = {}^b\mathbf{b} - {}^b\mathbf{om} \tag{4.8}$$

Substituting $^p\mathbf{om} = {}^b\mathbf{a} - {}^p\mathbf{am}$ to Equation 4.8 gives:

$$^p\mathbf{mb} = {}^b\mathbf{b} - {}^b\mathbf{a} - {}^p\mathbf{am} \tag{4.9}$$

Where OB is a vector of point B and is equal to $[b_x \quad b_y \quad b_z]^T$. Substitutions of known values into Equation 4.9 gives:

$$ {}^{p}\mathbf{mb} = \begin{bmatrix} mb_x \\ mb_y \\ mb_z \end{bmatrix} = \begin{bmatrix} b_x \\ b_y \\ b_z \end{bmatrix} + \begin{bmatrix} a_x \\ a_y \\ a_z \end{bmatrix} + \mathbf{R}_z(\gamma) \begin{bmatrix} r \\ 0 \\ 0 \end{bmatrix} \tag{4.10} $$

By using geometric similarities, values of α can be found as the summation of α_1 and α_2 and is expressed as:

$$ \alpha = 270^{\circ} - \alpha_1 + \alpha_2 \tag{4.11} $$

Where:

$$ \alpha_1 = \arccos\left(\frac{MB_{xy}}{\|MB\|}\right) \tag{4.12} $$

$$ \alpha_2 = \arccos\left(\frac{MB_z}{\|MB\|}\right) \tag{4.13} $$

Eventually, the unit vector in points C to B, denoted by $\hat{e}_{cb}$ is defined as follows:

$$ \hat{e}_{cb} = \mathbf{R}_y(-\alpha)\hat{e}_z \tag{4.14} $$

Where $\hat{e}_z$ is the unit vector along the z-axis.

4.2. Reconfigurable Planning

The position of contact points of each pulley is designed to be reconfigurable. This is to ensure that the robot will always be in dynamic equilibrium while fulfilling the given trajectory. The reconfigurability criteria are

based on cable tension and velocity. Both are treated as the objective function to be minimized. Two sets of constraints are also imposed on this problem. Therefore, it is treated as an optimization problem which can be mathematically expressed as:

$$\begin{gathered} minimize\ f(\mathbf{t},\tau) = norm(\mathbf{t},\tau) \\ subject\ to \\ 1.\tau > 0\ {}^{N}/_{m^2} \\ 2.\varepsilon_i < 10^{-3} \end{gathered} \tag{4.15}$$

The positions of each of the pulleys and angles γ are shown in Figure 4.3. The reconfigurable pulley angle γ_i for each exit point A_i has its range of rotations denoted as θ, and the relationship between γ_i and θ are as follows :

$$\begin{gathered} \theta = 0^{\circ}\ to\ 90^{\circ} \\ \gamma_1 = \theta + 90^{\circ} \\ \gamma_2 = \theta + 180^{\circ} \\ \gamma_3 = \theta + 270^{\circ} \\ \gamma_4 = \theta \end{gathered} \tag{4.16}$$

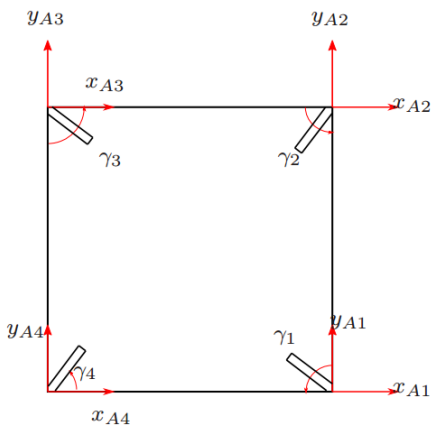

Figure 4.3. Top view of the CDPR Platform

4.3. Design Problem Formulation

The derivations of geometric, kinematic, and dynamic modeling of CDPR with the influence of pulley mechanisms are simulated through three different trajectories. Both design parameters and trajectory parameters for the base frame, the moving frame, and the pulleys, along with types of cable arrangements and reconfigurability are explained in the detail throughout this section.

4.3.1. Base Frame

The design parameters for the base frame are stated in Table 4.1. It consists of the general dimensions of the cube fixed frame (length, width, and height) and also the positions of each exit point in the base frame. Note that the exit points are situated on each connection of pulleys to the base frame.

Table 4.1. Design Parameters of the Base Frame

Base Frame				
No	Parameter	Symbol	Value	Note
1	Length	l_b	0.8 m	
2	Width	w_b	0.8 m	
3	Height	h_b	0.8 m	
9	Exit Points 1	$\mathbf{a}_1$	$[0.4 \quad -0.4 \quad 0.8]^T$ m	
10	Exit Points 2	$\mathbf{a}_2$	$[0.4 \quad 0.4 \quad 0.8]^T$m	
11	Exit Points 3	$\mathbf{a}_3$	$[-0.4 \quad 0.4 \quad 0.8]^T$m	
12	Exit Points 4	$\mathbf{a}_4$	$[-0.4 \quad -0.4 \quad 0.8]^T$m	

4.3.2. Moving Frame

The design parameters for the cube moving frame are described in Table 4.2. Note that the robot is designed to have only translational movements. Therefore, the yaw, pitch, and roll angles are equal to 0°. Also, the payload is situated on the moving platform's center of gravity, which leads to no moments due to the payload placement ($m_x = m_y = m_z = 0\ Nm$).

Table 4.2. Design Parameters of the Moving Frame

Moving Frame				
No	Parameter	Symbol	Value	Note
4	Length	l_p	0.1 m	
5	Width	w_p	0.1 m	
6	Height	h_p	0.1 m	
13	Anchor Points 1	$\mathbf{b}_1$	$[0.05 \quad -0.05 \quad 0.1]^T$m	
14	Anchor Points 2	$\mathbf{b}_2$	$[0.05 \quad 0.05 \quad 0.1]^T$m	
15	Anchor Points 3	$\mathbf{b}_3$	$[-0.05 \quad 0.05 \quad 0.1]^T$m	
16	Anchor Points 4	$\mathbf{b}_4$	$[-0.05 \quad -0.05 \quad 0.1]^T$n	
20	Payload	m	100 kg	

4.3.3. Pulley Parameters

The pulleys in the robot can move. It is set to be reconfigurable, based on constraints in reconfigurable planning on subchapter 4.2. The joint angle and limitations of the pulleys and the reconfigurable parameters are shown in Table 4.3. and 4.4, respectively.

Table 4.3. Design Parameters for Reconfigurable Pulleys

Pulley Design Parameters				
No	Aspects	Symbol	Value	Notes
1	Pulley Diameter	r_p	0.016 m	
2	Pulley Angle radius		$0^\circ - 90^\circ$	With respect to the pulley frame

Table 4.4. Reconfigurable Pulley Parameters

Pulley Type	Pulley Angle	Note
Fixed	45°	
Reconfigurable	$0^\circ - 90^\circ$	With respect to the pulley frame, 5° increment

4.3.4. Cable Arrangements

Two cable arrangements are used interchangeably for each trajectory. These arrangements are named standard and crossing arrangement, as shown in Figure 4.4.(a) and Figure 4.4.(b) respectively. It is based on the research on optimum cable arrangements for a suspended cable robot carried out by Hanafie et al. (Hanafie, Nurhami, Caro, & Pramujati, 2018). The research suggests that the crossing arrangement will give a bigger workspace compared to other cable arrangements. The standard arrangement is the conventional cable robot arrangement, where each exit point A_i is connected to anchor point B_i, with the same index. For instance, A_1 is connected to B_1, A_2 is connected to B_2, etc. On the other hand, the crossing arrangement is described when each of the odd - indexed exit points A_i is connected to the even indexed anchor point B_i. For instance, exit points A_1 is connected to B_2, exit points A_2 is connected to B_1, and so on. The detailed configuration is shown in Table 4.5.

Table 4.5. Connections for Each Cable Arrangements

Cable Arrangement	Configuration	Note
Standard	$A_1 \rightarrow B_1$ $A_2 \rightarrow B_2$ $A_3 \rightarrow B_3$ $A_4 \rightarrow B_4$	Based on the works of Hanafie et al (Hanafie, Nurhami, Caro, & Pramujati, 2018)
Crossing	$A_1 \rightarrow B_2$ $A_2 \rightarrow B_1$ $A_3 \rightarrow B_4$ $A_4 \rightarrow B_3$	

(a) (b)

Figure 4.4. (a) Standard (b) Crossing Arrangement

4.4. Trajectory Simulation Result

Three trajectories are used to simulate the behavior of CDPR under the influence of the pulley mechanism (Gosselin, Global Planning of Dynamically Feasible Trajectories for Three-DOF Spatial Cable-Suspended Parallel Robots, 2012). These trajectories are sinusoidal motion, circular horizontal, and vertical helix. Each trajectory is simulated with two cable arrangements, the standard and crossing arrangement. Through these simulations, graphs on cable tensions, cable velocity, error, and pulley angles are obtained. These graphs will be used to analyze the behavior of CDPR under dynamic trajectories.

4.4.1. Sinusoidal Motion

The trajectory parameters used to simulate the sinusoidal motion are shown in Table 4.6., whereas the visualization of the trajectory with respect to the Z-Axis is shown in Figure 4.5.

Table 4.6. Trajectory Parameters of the Sinusoidal Motion

p_x (m)	p_y (m)	p_z (m)	r (m)	$\omega(rad/s)$	z_0 (m)
0	0	z_0	0.1	1	0.4

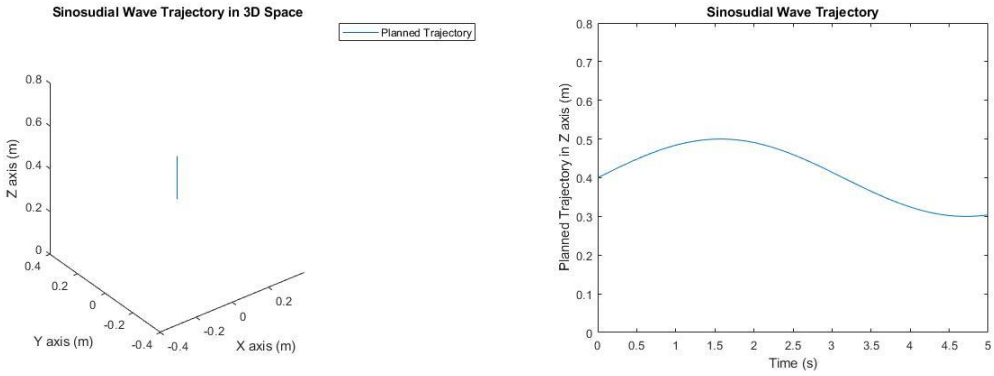

(a) Sinosudial Wave in 3D Space (b) Sinosudial Wave with respet to Time

Figure 4.5. Planned Sinosudial Wave of the Robot

The numerical results of the standard arrangement under sinusoidal motion are shown in Table 4.7. The comparisons are carried out for two types of configuration, namely non – reconfigurable robot when $\gamma_i = 45^\circ$ and reconfigurable ones. For both non – reconfigurable and reconfigurable robot, four graphs are obtained, namely tension distribution (τ_i), pulley angle (γ_i), error (ε_i) and cable velocity $(\dot{l}_i)$.

It is shown that the tensions for the non-reconfigurable pulley $(\gamma_i = 45^\circ)$ cannot meet the tension requirements $(\tau_i < 0N)$. The calculated error is $\varepsilon_i = 14 \times 10^{-4}$ at maximum, with maximum cable velocity at $\dot{l}_i = 0.06\ {}^{m}/_{s}$. The reconfigurable pulleys can give better tensions performance as each cable tension is positive but does not meet the required error ε_i. This tension distribution can be realized when the pulleys are arranged into $\gamma_1 = \gamma_2 = 0°$, $\gamma_3 = 10°$ and $\gamma_4 = 15°$. The maximum error at the feasible time frame are $\varepsilon_i = 0.026$ with maximum cable velocity at $\dot{l}_i = 0.0613\ {}^{m}/_{s}$.

Table 4.7. Result of Sinusoidal Motion using Standard Arrangement

Aspects	Fixed Pulley	Reconfigurable
τ	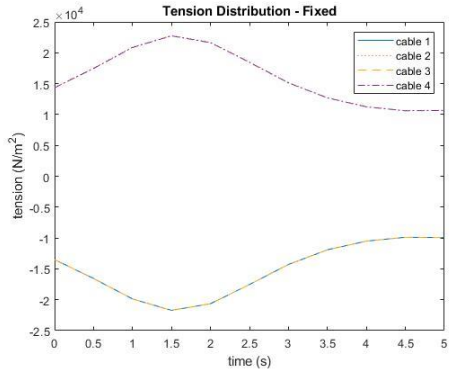	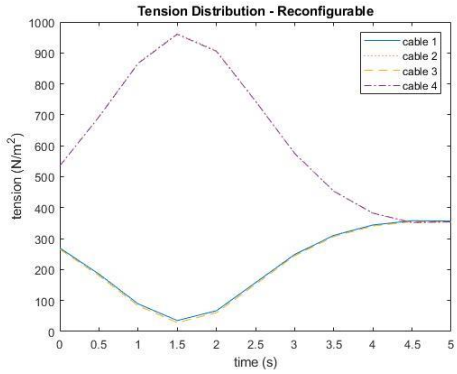
γ	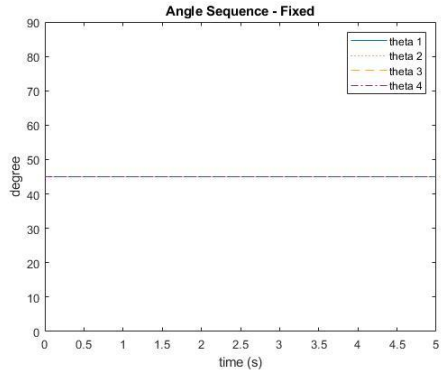	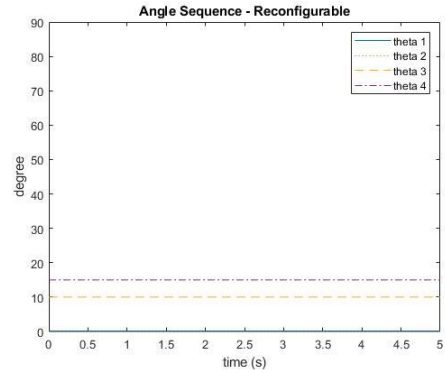
$\dot{\imath}$	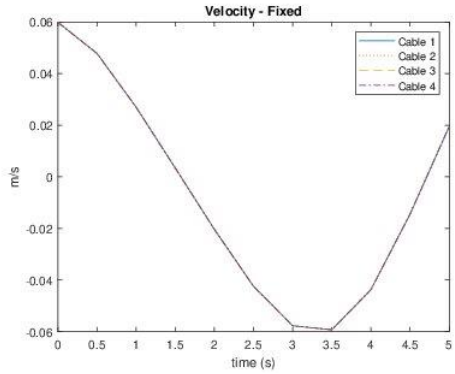	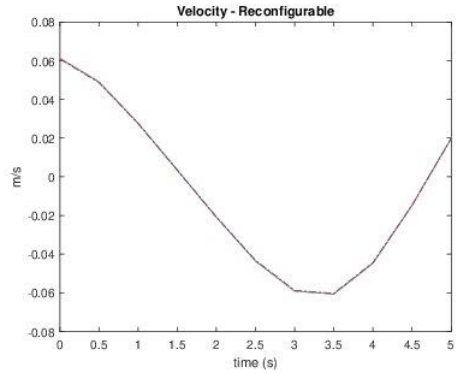
ε	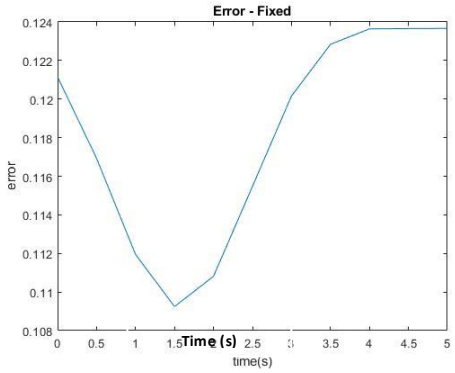	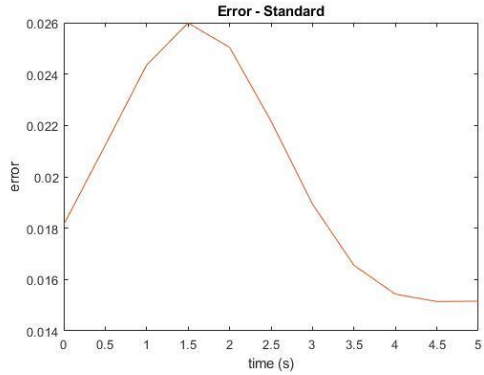

For the crossing arrangement, the non-reconfigurable and reconfigurable pulleys are also studied and compared as shown in Table 4.8. The tension distribution τ_i for both non-reconfigurable and reconfigurable pulley remains positive, although the tension distribution of reconfigurable pulley is slightly lower than the non-reconfigurable one. The maximum tension value for the reconfigurable pulleys is $555\ N$. The least tension which can be achieved by this arrangement is when the pulleys are assembled to be $\gamma_1 = \gamma_2 = \gamma_3 = \gamma_4 = 0°$. The error generated from the reconfigurable pulleys is lower than to the non-reconfigurable one. The cable velocity for both non – reconfigurable are slightly lower than the reconfigurable pulleys with maximum and minimum velocity for the respective configurations are at $\pm 0.547\ {}^{m}/_{s}$ at $t = 0\ s$ and $\pm 0.550\ {}^{m}/_{s}$ at $t = 3.5\ s$ respectively

Table 4.8. Result of Sinusoidal using Crossing Arrangement

Aspects	Fixed Pulley	Reconfigurable
τ	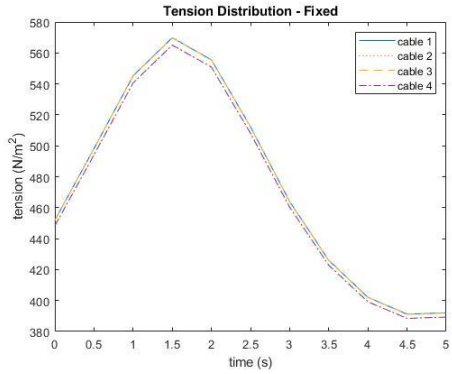	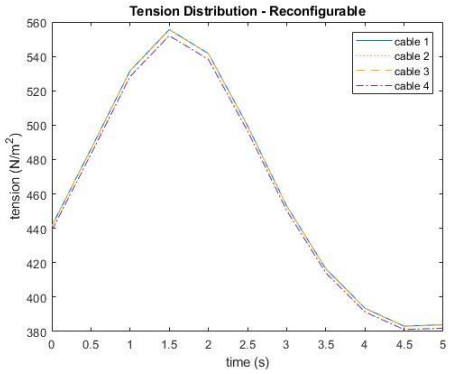
γ	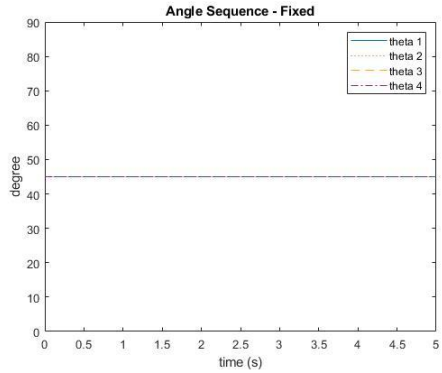	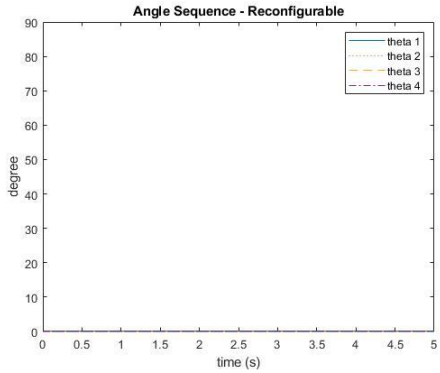
$\dot{\imath}$	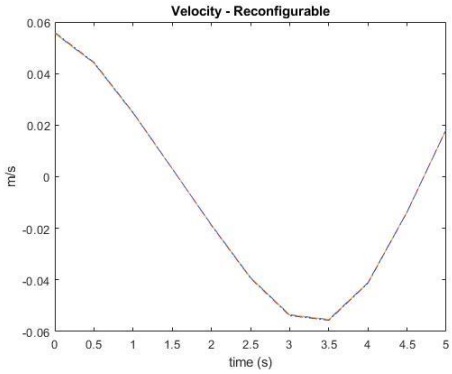	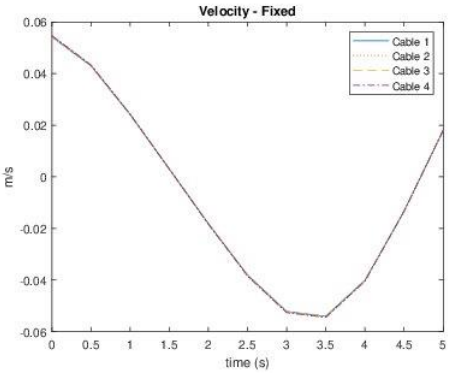
ε	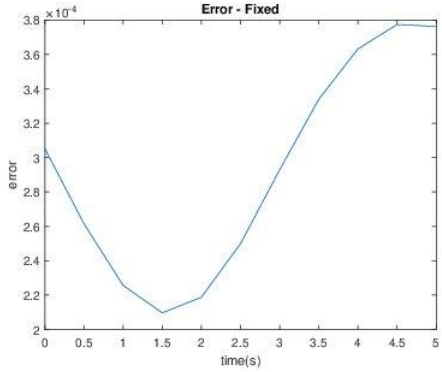	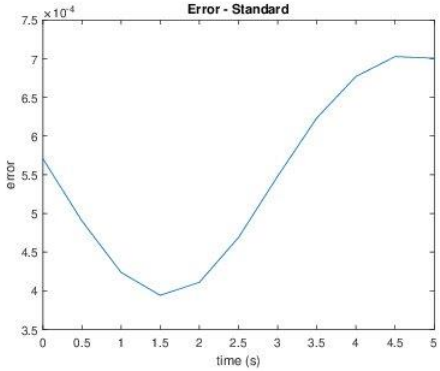

4.4.2. Vertical Helix

The trajectory parameters used to simulate the vertical helix are shown in Table 4.9., whereas the visualization of the trajectory with respect to the Z-Axis is shown in Figure 4.6.

Table 4.9. Trajectory Parameters of the Vertical Helix

p_x (m)	p_y (m)	p_z (m)	r (m)	z_0 (m)	h (m)	$\omega_1(rad/s)$	$\omega_2(rad/s)$
0	0	z_0	0.1	0.4	0.3	0.15	0.15

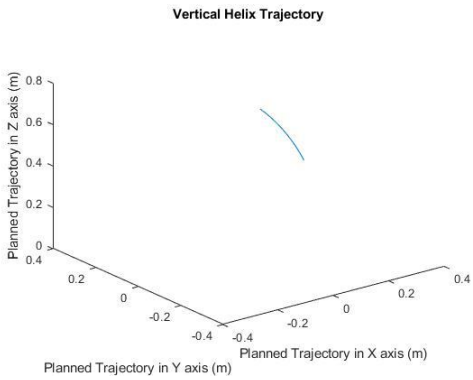

Figure 4.6. Planned Vertical Helix of the Robot

The results for the standard arrangement are shown in Table 4.10. There are four aspects to be observed, namely tension distribution (τ_i), pulley angle (γ_i), error (ε_i) and cable velocity $(\dot{l}_i)$. It is observed that the non – reconfigurable pulley is not able to give positive tension distribution, whereas the reconfigurable pulley can produce positive tension although only from $t = 3.2\ s$ to $t = 5\ s$. The positive tension can be achieved by the robot when the pulley is assembled to be $\gamma_1 = 0°$, $\gamma_2 = \gamma_3 = 10°$ and $\gamma_4 = 50°$. The reconfigurable pulley has a lower error if compared to the non – reconfigurable one. The maximum error for the reconfigurable pulley has a lower error if compared to the non – reconfigurable one. The maximum error for the reconfigurable pulley is $\varepsilon = 1.325$, whereas the maximum error for the non – reconfigurable pulley is $\varepsilon = 1.54$. It is noteworthy that the error values for both non – reconfigurable pulleys are above the stated error requirements. The values of cable velocities for the reconfigurable system are lower

if compared to the non – reconfigurable pulley. The maximum value of the cable velocity of the reconfigurable system is $\dot{l}_i = 0.0388\ {}^{m}/_{s}$, whereas the maximum value of cable velocity of the non – reconfigurable pulley system is $\dot{l}_i = 0.0514\ {}^{m}/_{s}$.

Table 4.10. Result of Vertical Helix using Standard Arrangement

Aspects	Fixed Pulley	Reconfigurable
τ	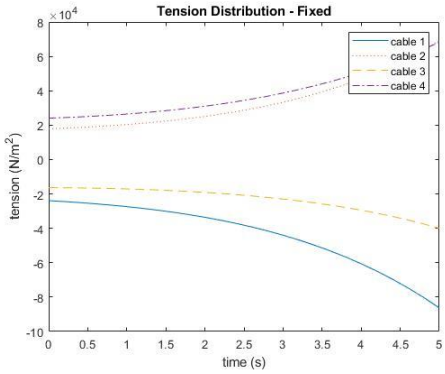	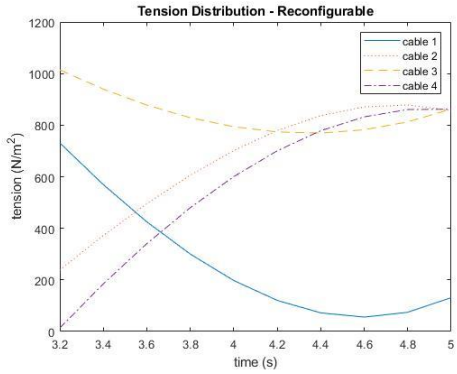
γ	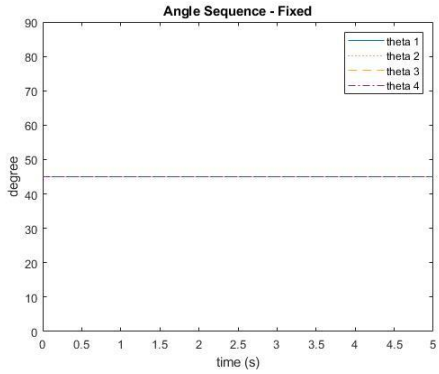	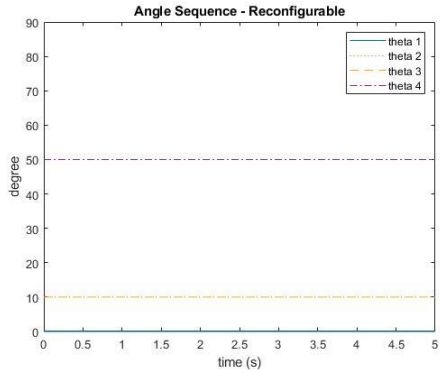
$\dot{\mathbf{l}}$	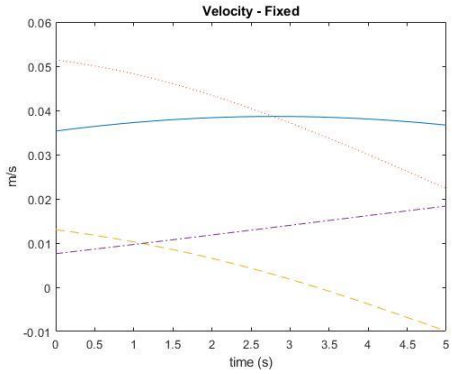	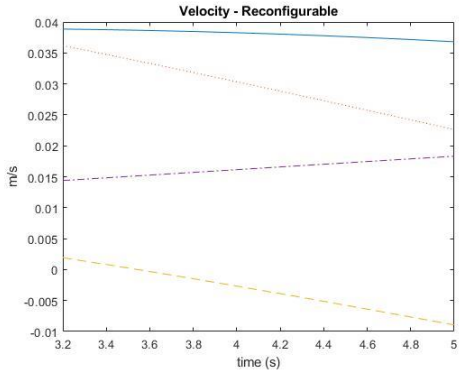
ε	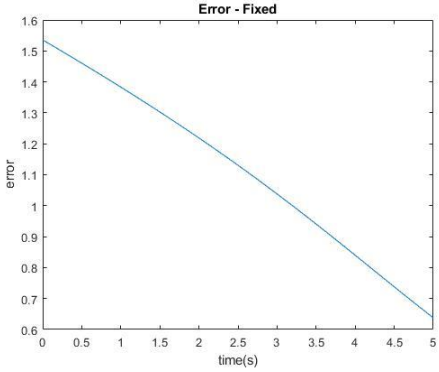	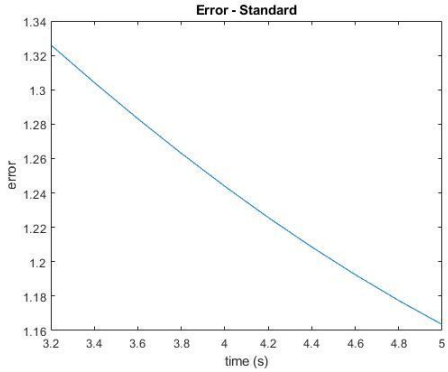

The crossing arrangement is also studied for the vertical helix as shown in Table 4.11. It is observed that the tension and cable velocity for both non – reconfigurable and the reconfigurable pulleys are almost identical. However, the tensions and cable velocities of the reconfigurable pulley are slightly lower than the non – reconfigurable ones. These tensions are achieved if the pully is assembled to $\gamma_1 = \gamma_2 = 0, \gamma_3 = 10°$ and $\gamma_4 = 50°$. The errors for non – reconfigurable pulley are slightly lower, e.g. $\varepsilon = 1.075$, than the reconfigurable pulley, e.g. $\varepsilon = 1.01$. It means that the crossing arrangement fives better tension if compared with the standard arrangement along the trajectory of the vertical helix. The cable velocity for both reconfigurable and non – reconfigurable pulleys are almost identical, although the reconfigurable pulleys have a higher value.

Table 4.11. Result of Vertical Helix using Crossing Arrangement

Aspects	Fixed Pulley	Reconfigurable
τ	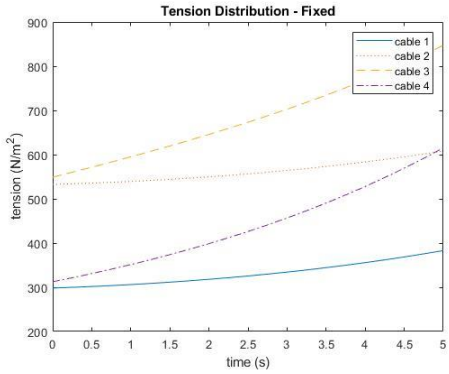	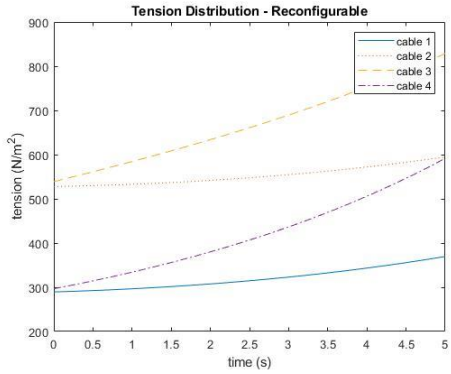
γ	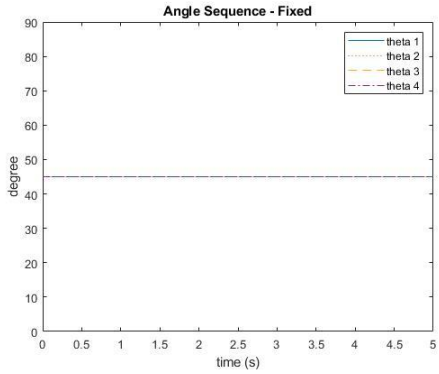	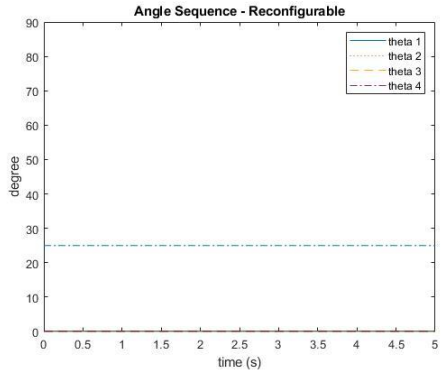
t	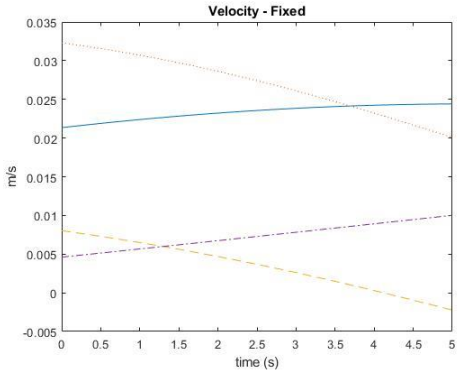	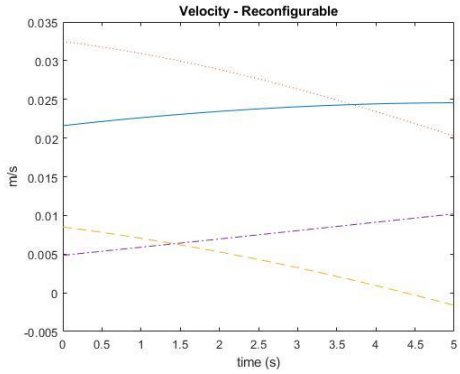
ε	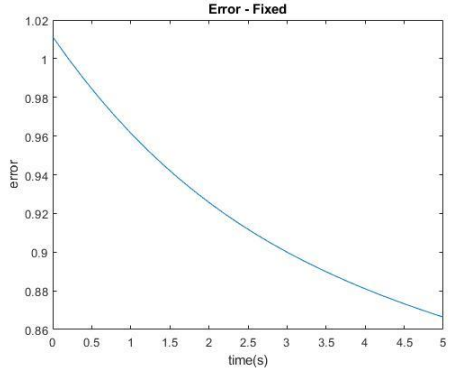	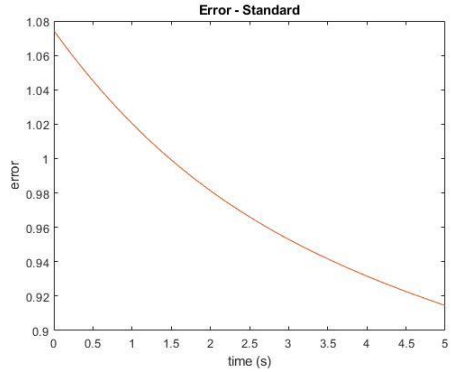

4.4.3. Summary

From these simulations, it can be observed that:

1. The fixed pulleys are unable to follow all trajectories because of negative tension, whereas reconfigurable pulleys can give positive tensions throughout the trajectory.
2. When the standard arrangement is equipped with reconfigurable pulleys, the overall tension distributions are significantly improved.
3. When using the crossing arrangement, both the fixed pulleys and the reconfigurable pulleys give almost identical results in tension distribution, although the reconfigurable pulleys give slightly lower values.

The knowledge obtained from mechanical modeling is used to design the control system of the cable robot.

4.5. Control System

The robot is designed to move debris due to natural disasters. Therefore, it does not need to be in high precision. Also, the actuator needs to be able to bear high loads from the debris. One challenge when controlling the cable robot is that the flexible nature of cables which can only exert force introduces a crucial constrain to the control system. The position of the moving platform is harder to control due to its flexibility, which leads to lower accuracy (Jung et al., 2016). The need to be in tension also implies that under - constrained configuration cannot be fully controlled (Qian et al., 2018). Most of the developed control schemes stated in the literature review use sensor to read its set points. Sensors are prone to noises, do not work well on long ranges, and needs to be calibrated. Furthermore, having sensors can slow the assembly process. This will not work well since the search and rescue robot needs to be deployed with ease and speed. One of the alternatives to substitute the use of sensors is by using stepper motors as actuators.

Stepper motor moves discretely. This can be advantageous since it does not need a sensor to read the set-point. These facts served as the base to develop a model-based control algorithm will be presented for the suspended cable robot.

4.5.1. Conversion into motor set points

The cable lengths obtained from the geometric model needs to be represented in terms of its actuators. In this case, stepper motors are used to drive the cables. Stepper motors are chosen because it moves by the number of steps, which is the multiplication of its step angle. Therefore, actual steps can be gathered without the need for additional sensors. Before deriving this relationship, some assumptions are considered as follows:

1. Pulley and cables are assumed mass-less, and friction between pulley and cables are assumed negligible
2. Winches are assumed to always coil only one layer of cable
3. Transmission loss within the actuator is assumed negligible
4. No missed steps generated by the stepper motor

The current control scheme applied to the robot focuses solely on position control. The rotation of the shaft angle acts as the setpoint to the control scheme. The stepper motor moves the shaft to the desired angle θ_{shaft}, determined by the number of steps n_m that must be generated according to its step angle θ_a, mathematically expressed as:

$$\theta_{shaft} = n_m \theta_a \tag{4.17}$$

Moreover, the relationship between the desired cable length l_{des} and the desired shaft angle can be expressed as:

$$\theta_{shaft} = \frac{l_{des}}{r_{shaft}} \tag{4.18}$$

where r_{shaft} defined the shaft radius. Hence, the number of steps required to generate the desired shaft angle based on the desired cable length can be mathematically expressed as:

$$n_m \theta_a = \frac{l_{des}}{r_{shaft}} \tag{4.19}$$

Rearranging the equation to find the number of steps n_m gives:

$$n_m = \frac{l_{des}}{r_{shaft}\theta_a} \tag{4.20}$$

4.5.2. Proposed Control Scheme

The term model-based refers to the use of the actuator model in the control algorithm. Stepper motor is used to drive the cables, with the number of steps taken as set points. The discrete nature of moving in steps is used as feedback to the system. Therefore, the cable lengths can be calculated by using the linear - angular relationship between cables and stepper motor. The desired and actual trajectory will be compared along with its error. An improvement will be proposed based on this result.

The Block diagram is comprised of two subsystems, which are the reference model and implemented control. The mechanical modeling of the whole system, from the robot model to its supporting mechanisms, is carried out in the reference model. The reference model converts the desired trajectory from Cartesian space into the joint space. The Cartesian trajectory itself is derived with reference to the works of Gosselin (Gosselin, 2012). The trajectory serves as input for geometric analysis, carried out to convert the desired position into the desired cable lengths. It is then translated into the number of steps that must be generated by the stepper motor. The proposed block diagram of the system is shown in Figure 4.7.

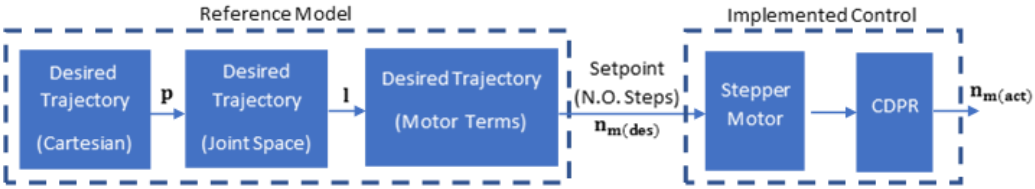

Figure 4.7. Block Diagram for the Entire System

4.5.1.1. Stepper Motor General Block Diagram

The general block diagram for each stepper motor is shown in Figure 4.6. The block diagram is applicable for both position and velocity control.

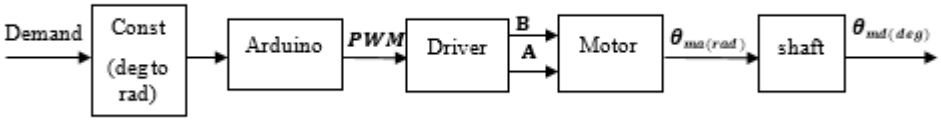

Figure 4.8. Block Diagram for Individual Stepper Motor

Each cable will be driven by a SUMTOR 57HS6425A4D8 stepper motor. The specification of the stepper motor is shown in Table 4.12.

Table 4.12. Motor Specification

Aspects	Value
Phase	2
Step Angle (deg)	1.8
Current / Phase (A)	2.5
Inductance (mH)	4.5
Rotor Inertia	380
Holding Torque (N.cm)	1.5
Detent Torque (N.cm)	5

4.5.3. Design and Trajectory Parameters

The results on position (desired versus actual) and error will be presented for each trajectory. The values assigned for each design parameter are shown in Table 4.13.

Table 4.13. Design Parameters

l_b (m)	w_b (m)	h_b (m)	l_p (m)	w_p (m)	h_p (m)	r_{shaft} (m)	*Payload* (kg)
0.8	0.8	0.8	0.1	0.1	0.1	0.005	1

4.6. Control Simulation Result

The control scheme is simulated into three trajectories, namely the sinusoidal motion, the circular trajectory, and the vertical helix. For each trajectory, a comparison between the desired and the simulated trajectory will be presented, along with its behavior and error for each axis.

4.6.1. Sinusoidal Motion

The trajectory parameters used to simulate the sinusoidal motion are shown in Table 4.14.

Table 4.14. Trajectory Parameters for the Sinusoidal Motion

p_x (m)	p_y (m)	p_z (m)	z_0 (m)	$\omega(rad/s)$
0	0	z_0	0.2	1

The comparison between actual and desired pose on the sinusoidal wave is shown in Figure 4.9. It is observed in Figure 4.9(a) that there is a considerable difference between the setpoint and the actual position when performing the downward motion. The observable error on the bottom of each valley of the sinusoidal wave is as high as 0.2 m, which resulted in an error of 26% on average as shown in Fig. 4.9(b).

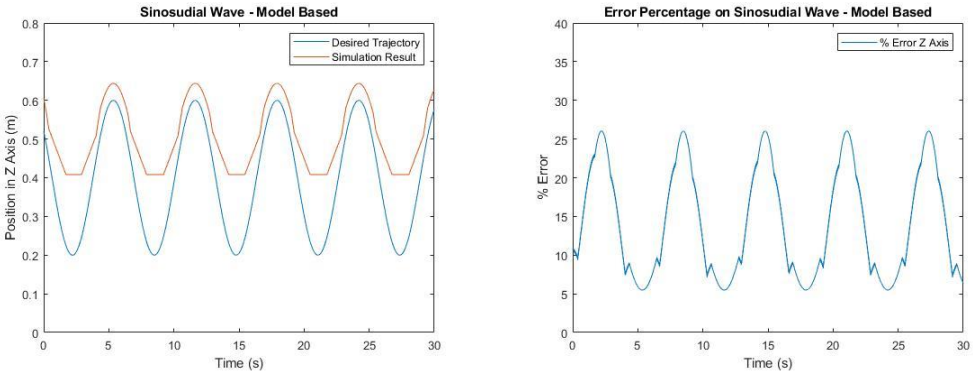

(a) Desired vs Actual Pose (b) Position Error

Figure. 4.9. The result on Model-Based Controlled Scheme with Sinusoidal Motion

4.6.2. Circular Trajectory

The trajectory parameters used to simulate the circular trajectory are shown in Table 4.15.

Table 4.15. Trajectory Parameters for Circular Trajectory

p_x (m)	p_y (m)	p_z (m)	r (m)	$\omega(rad/s)$	z_0 (m)
0	0	z_0	0.2	0.5	0.5

The comparison between the actual and desired trajectory while using the model-based control scheme is shown in Figure. 4.10(b). Notice that the actual trajectory has a smaller radius and higher position than the desired trajectory. Its pose breakdown with respect to each axis is summarized in Table 4.16. It is observed that the difference in its circular radius for both x and y-axis is at 0.023 m. The highest error for each axis is at 9.5% and 14.2%, respectively. There is a significant gap between the desired and actual pose in the z-axis of 0.12 m, which resulted in an error of 14.9%.

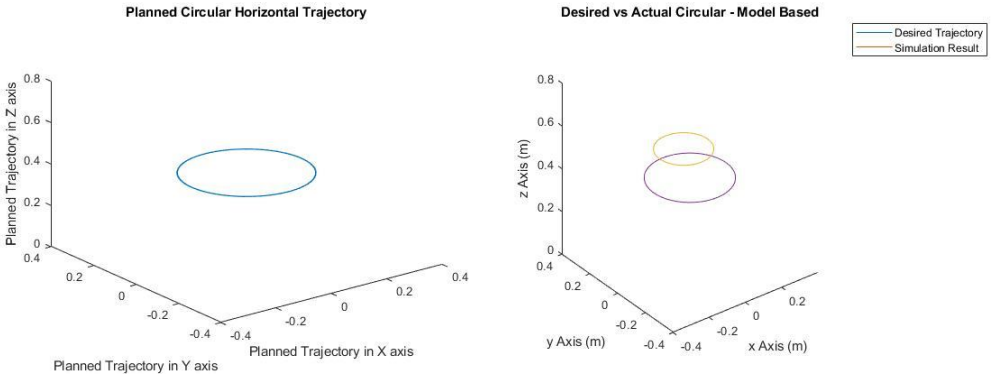

(a) Planned Trajectory (b) Desired versus Actual

Figure 4.10. Model-Based Control with Circular Trajectory

Table 4.16. Decomposition of Circular Trajectory with respect to each axis

Axis	Trajectory	Error
x	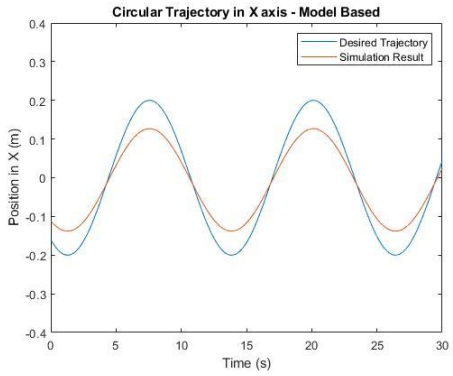	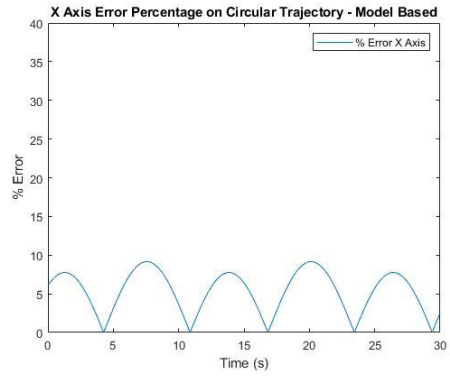
y	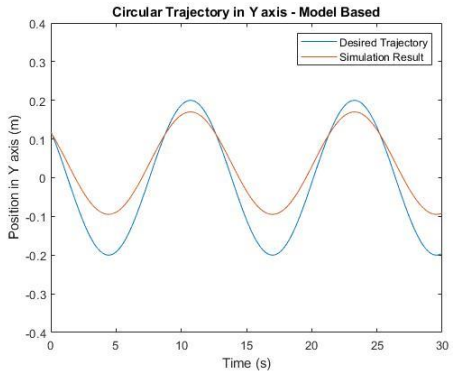	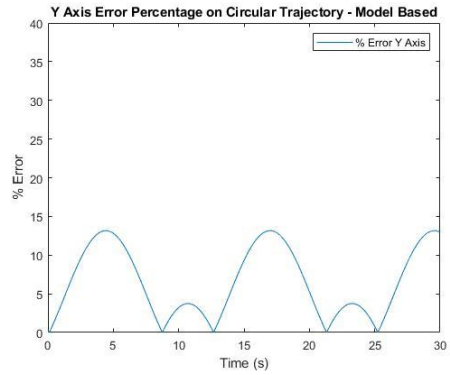
z	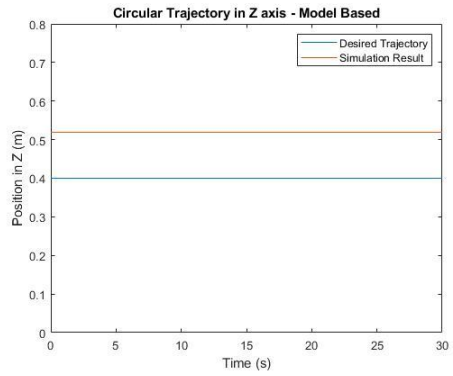	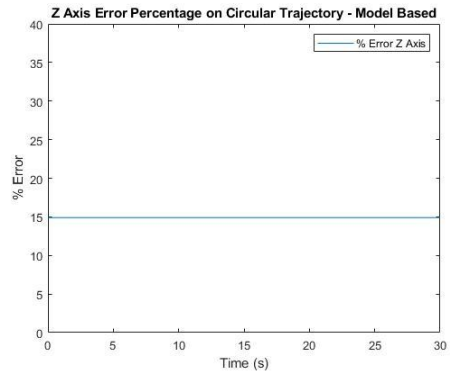

4.6.3. Vertical Helix

The trajectory parameters used to simulate the vertical helix are shown in Table 4.14.

Table 4.17. Trajectory Parameters for Vertical Helix

p_x (m)	p_y (m)	p_z (m)	r (m)	z_0 (m)	h (m)	$\omega_1(rad/s)$	$\omega_2(rad/s)$
0	0	z_0	0.02	0.4	0.3	0.5	0.5

The Comparison between the desired and actual trajectory for vertical helix is shown in Fig. 4.11(b). The results on each axis are summarized in Table 4.18. Note that the actual trajectory has a smaller radius and higher position than the desired trajectory. There is a slight difference between the desired and the actual pose in the *x* and *y*-axis, but in general, the *y*-axis performs better than the *x*-axis. In terms of error, the overall error is less than 5% and 5.5% for both axes, respectively. As for the *z*-axis, a major difference is seen between the desired and the actual pose, with error as high as 32.8%.

Based on these results, it can be concluded that in general, the control scheme performs well on the *x* and *y*-axis, but not on the *z*-axis. Therefore, we proposed an improvement termed error compensation control scheme.

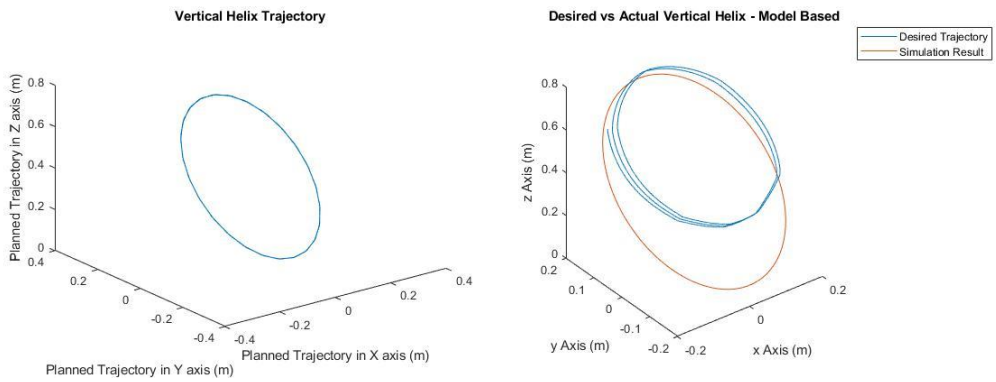

(a) Planned Trajectory (b) Desired versus Actual

Figure 4.11. Vertical Helix with Model-Based Control Scheme

Table 4.18. Decomposition of Vertical Helix with respect to each axis

Axis	Trajectory	Error
x	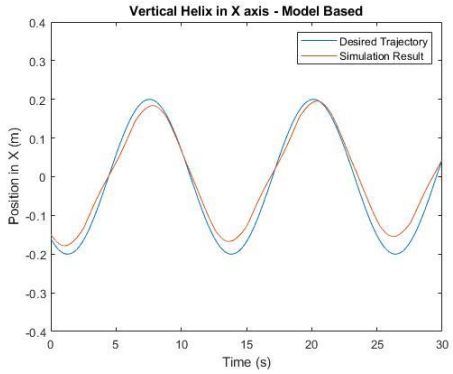	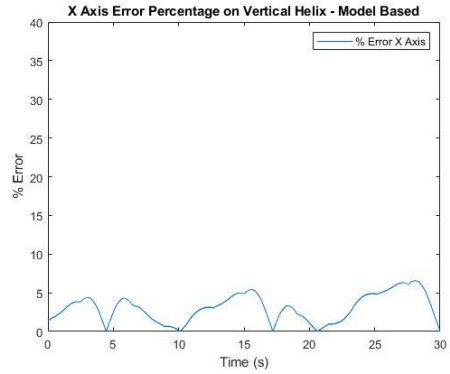
y	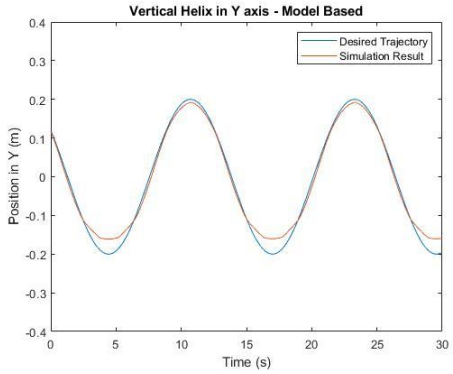	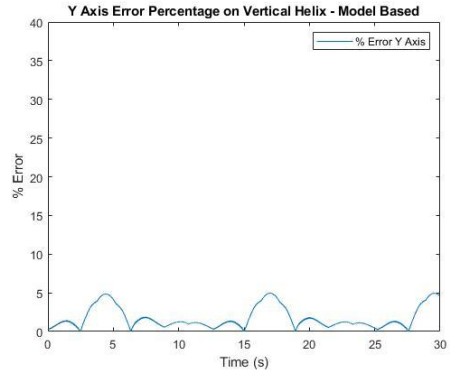
z	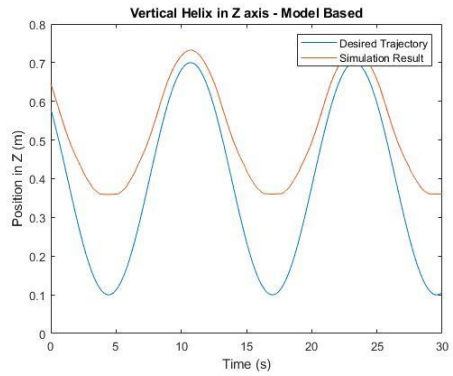	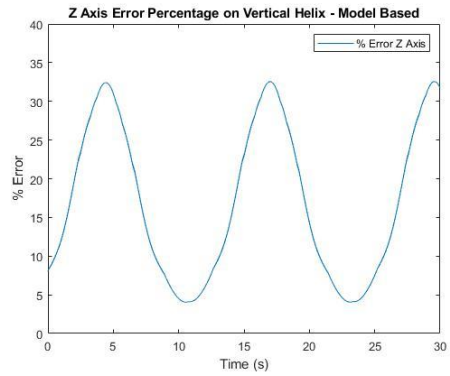

4.7. Improvement: Error Compensation Scheme

The error compensation scheme is an improvement to the previous control scheme. This control scheme is developed to increase the positional accuracy of the controller, especially in the *z*-axis. It is similar to the model-based scheme, but with its number of steps fed back through the system as actual cable lengths, as shown

in Figure 4.12. Multiplying the number of steps by the shaft radius will give the actual cable length, expressed as:

$$l_{act} = n_m r_{shaft} \theta_a \tag{4.21}$$

Routing this value back and subtracting this value with the desired cable length will result in a value that is similar to a position error. The error will be added to the system as an addition to find the compensated length, expressed as:

$$l_{comp} = l_{des} + error_{comp} \tag{4.22}$$

The difference between the actual and desired cable length is termed $error_{comp}$, which is mathematically expressed as:

$$error_{comp} = l_{act} - l_{des} \tag{4.23}$$

It is noteworthy that since the stepper motor moves in equal steps, only integer values are registered as valid input. But the conversion from cable length into the number of steps can result in decimal numbers. To accommodate the need to have integer input, the number of steps is either rounded up or down to the nearest integer number. Routing the actual number of steps will also eliminate error that arises from the conversion.

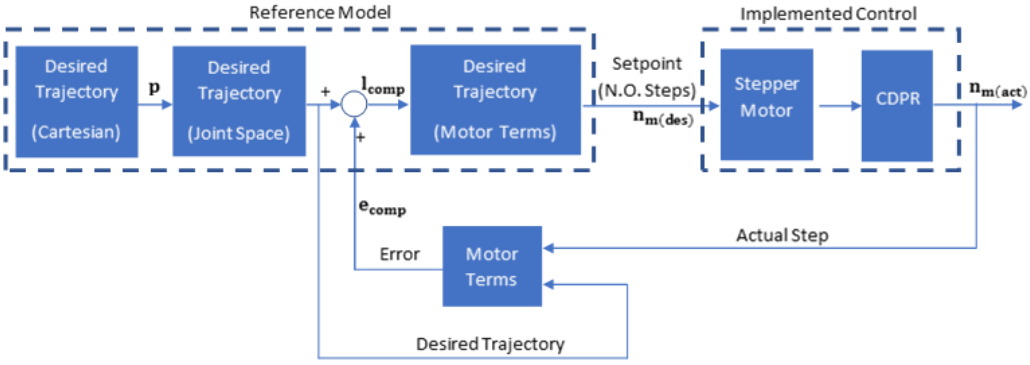

Figure 4.12. Proposed Compensation on the System

4.7.1. Sinusoidal motion

The results of sinusoidal motion with error compensation are shown in Figure 4.13. When the sinusoidal wave is carried out using the error compensation scheme, the robot performs better, as shown in Figure 4.13(b). There has been a considerable reduction in the overshoot, as shown in Figure 4.13(a). The position error is reduced by 44%, down from 26% to 14.5% on average. The rise in error to 22.6% on the first peak is due to the initial set up of the actuators matching the setpoint. The reduction is noticeably seen in the downward motion.

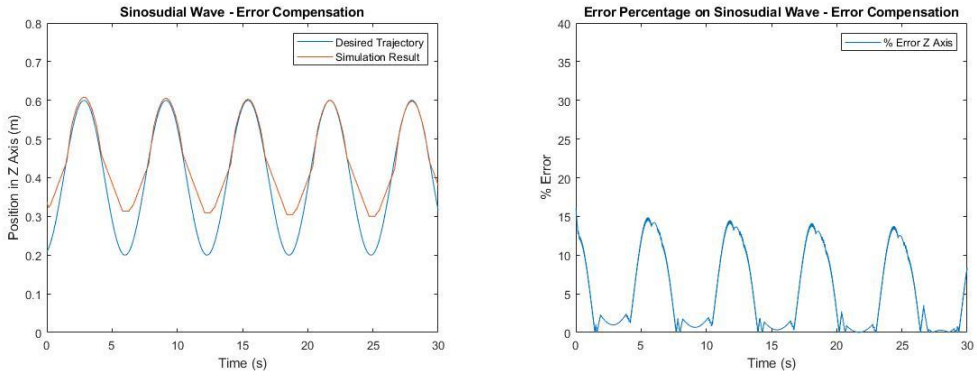

(a) Desired vs Actual (b) Position Error

Figure 4.13. Error Compensation Control scheme on Sinusoidal Motion

4.7.2. Circular Trajectory

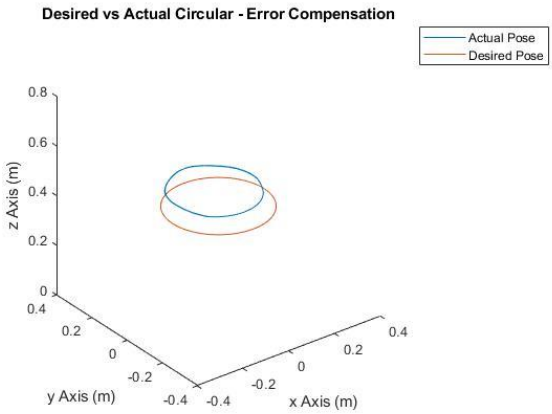

Figure 4.14. Desired versus Actual Pose during Circular Trajectory when using Error Compensator Control Scheme

Desired versus actual pose for the circular trajectory is shown in Figure 4.14. Overall, the controller able to follow the pose better in terms of its circular radius if compared to the previous control scheme. The Pose breakdown with respect to each axis is summarized in Table 4.19. Improvements are seen for all axis and noticeable especially in the z-axis. Both *x* and *y* have a considerable improvement in compliance, with a reduction in error of 50.5% and 62% to 5.3% and 5.7% respectively. In terms of the *z*-axis, the actual pose is significantly lower than before, with 52% reduction in error to 7.2% on average.

Table 4.19. Decomposition of Circular Trajectory with respect to each axis

Axis	Trajectory	Error
x	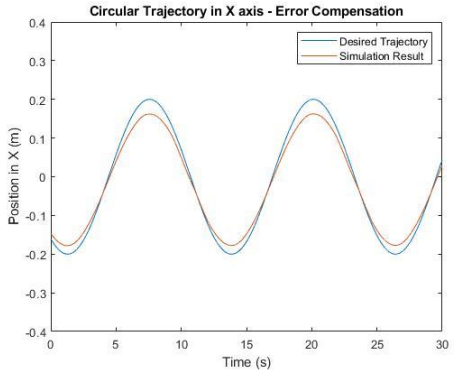	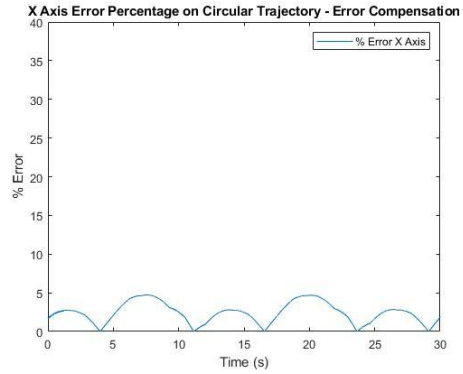
y	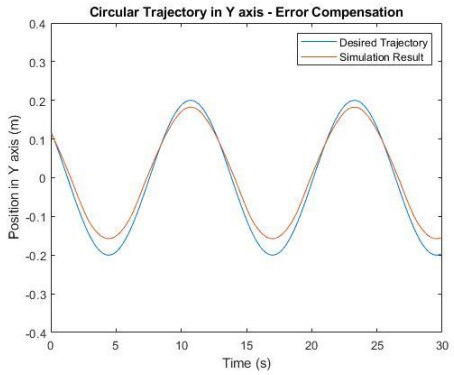	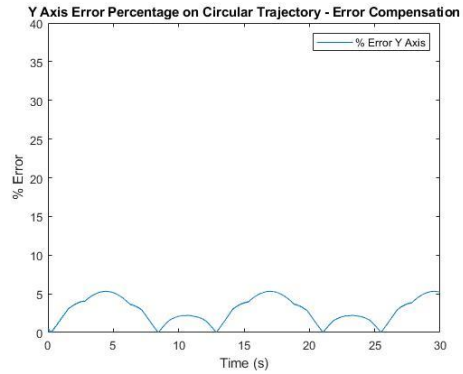
z	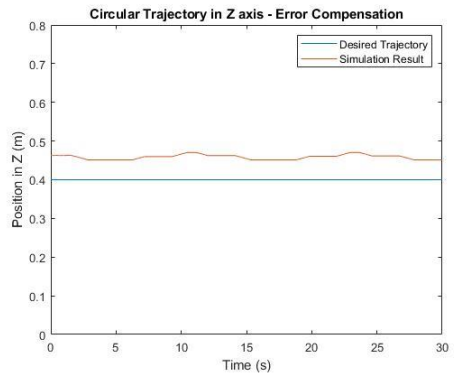	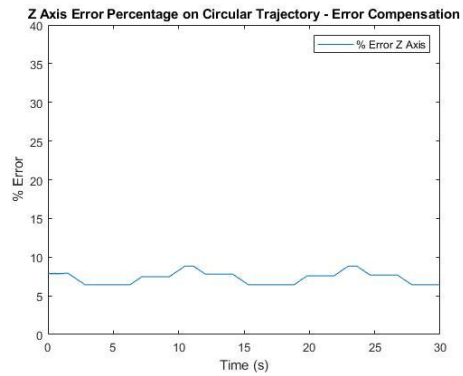

4.7.3. Vertical helix

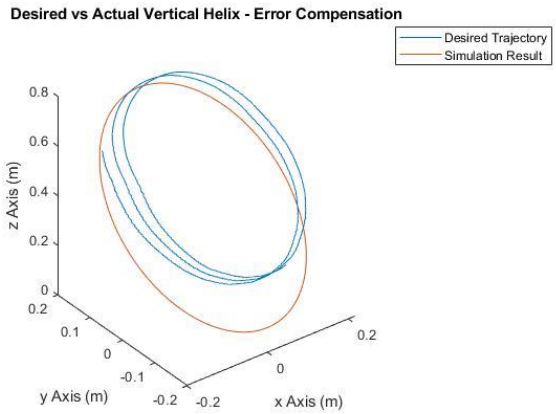

Figure 4.15. Desired versus Actual Pose during Vertical Helix when using Error Compensator Control Scheme

Significant improvement is seen in the vertical helix when using the error compensation scheme, as shown in Figure 4.15. The circular radius becomes wider and the robot able to follow the *z*-axis trajectory better. The trajectory for each axis is summarized in Table 4.20. Using the error compensation scheme reduces the error on the *y*-axis for 26%, but a slight increase of 29% to 7.1% for the *x*-axis. The error reduction is also seen on the *z*-axis of the vertical helix of 38.4%, from 32.5% to 20.5%. The highest error is still registered at the downward motion, especially in the lowest position.

Table 4.20. Decomposition of Vertical Helix with respect to each axis

Axis	Trajectory	Error
x	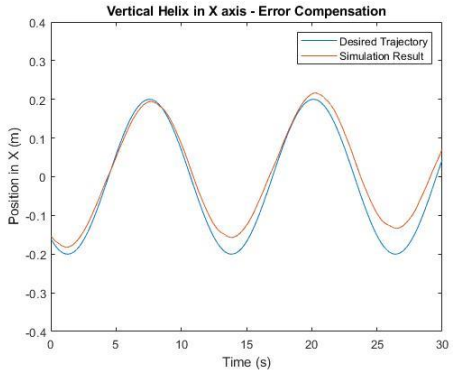	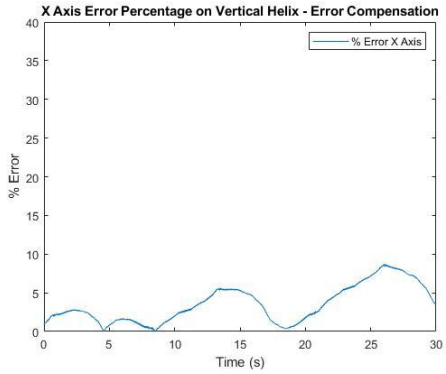
y	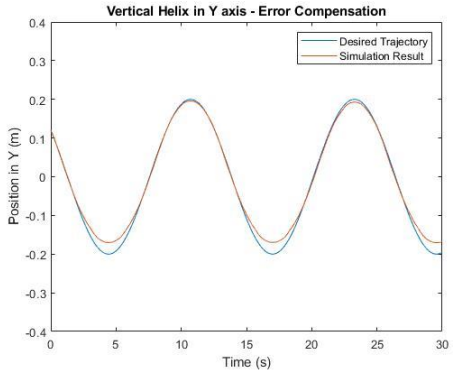	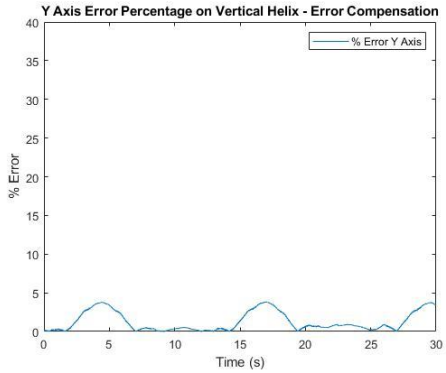
z	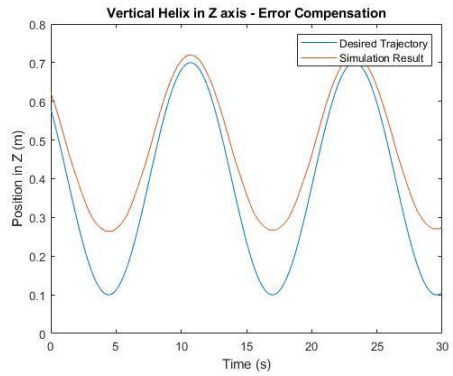	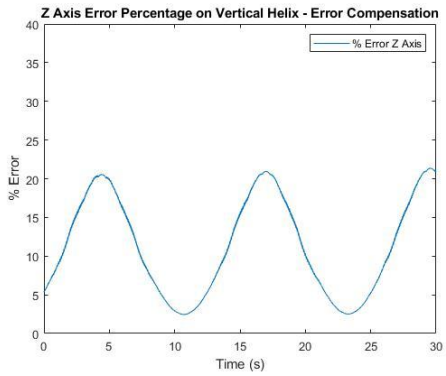

CHAPTER 5

CONCLUSIONS AND FUTURE WORKS

5.1. Conclusion

This thesis presents the development of a suspended cable-driven parallel robot. It is divided into two major scopes, mechanical modeling, and control system. The robot consists of a cube base and cube moving platform that are connected by four cables through the pulley mechanism. Cables run through these pulleys attached to winches in one end, which are driven by stepper motors, and moving platform at the other end.

5.1.1. Mechanical Modelling

Thanks to the pulley mechanisms which can be oriented independently, the robot reconfigurability can be realized. The inverse kinematics of cable and pulley were initially derived to represent cable tensions and the cable velocities through the dynamics affect the cable tensions and the cable velocities through the dynamic equilibrium analysis. Two robot structures were compared for two distinct parametric trajectories. During the reconfiguration, the cable tensions should always fulfill the dynamic equilibrium state and the minimum tension should not be null to avoid cable slack. Significant improvement in tension distribution is achieved through reconfigurable pulleys for robot structure A on both trajectories. Slight reduction in tension values are also achieved through reconfigurable pulleys for robot structure B. Overall, it is shown that additional reconfigurability ensures always positive tension throughout the trajectories.

5.1.2. Control System

A control scheme and its improvement for suspended cable-driven parallel robots have been developed, namely model-based and error compensation control. Both control scheme consists of two systems, namely the reference model and the

implemented control. The main difference between the model-based and error compensation control is that the latter uses the nature of the stepper motor to acquire the actual cable length, without the need to use sensors. Both schemes are tested to three trajectories, sinusoidal, circular, and vertical helix. In general, the model-based control scheme performs better in the *x* and *y*-axis, but not in the *z-axis*. The error in the *z*-axis is as high as 32.5% when performing the vertical helix. The error compensation scheme can perform better than the model-based ones, reducing error for all trajectories, noticeably in the *z*-axis. The reduction in error for the *z*-axis is reduced by 44%, 52%, and 38.4% for sinusoidal, circular, and vertical helix, respectively.

5.2. Publications Output

This research has resulted in several publications, described as follows :

1. Handojo, V. A, Syamlan, A.T., Nurhami, L.,Pramujati, B., Wasiwitono, U., 2018. *Cable Driven Parallel Robot with Big Interference-Free Workspace.* Mechanism and Machine Science Select Proceedings of Asian MMS 2018. Bengaluru.

2. Syamlan, A. T., Nurahmi, L., Pramujati, B. & Tamara, M. N., 2019. *Dynamic Trajectory Generation of Suspended Cable-Driven Parallel Robot.* Jogjakarta, AIP.
3. Syamlan, A. T., Nurahmi, L., Tamara, M. N. & Pramujati, B., 2020. Dynamic Trajectory Planning of Reconfigurable Suspended Cable Robot. *International Journal of Dynamics and Control,* 8(2).
4. Syamlan, A. T., Pramujati, B., Nurahmi, L. & Tamara, M. N. 2020. Model-based Control Algorithm for Search-and-Rescue Cable-Driven Parallel Robot. Journal of Robotics (Submitted)

5.3. Future Works

Several improvements is suggested based on this research, namely:

1. Sensors should be added into the prototype to enable more advanced control system, such as torque control
2. Cable stiffness should be calculated and accounted into the dynamic analysis
3. Reconfigurability should be applied to the prototype
4. The supporting mechanisms, especially winches, should be designed to increase the accuracy of the current control system
5. The vibration of the cables should be incorporated.

(This page is left intentionally blank)

REFERENCES

Albus, J., Bostelman, R. and Dagalakis, N. (1993), "The NIST Robocrane", *Journal of Robotic Systems,* Vol. 10, No. 5.

Alp, A. B. and Agrawal, S. K. (2002), "Cable Suspended Robots: Feedback Controllers with Positive Inputs", *Proceedings of the 2002 American Control Conference (ACC).* pp. 815-820.

Baklouti, S., Courteille, E., Caro, S., and Dkhil, M. (2017), "Dynamic and Oscillatory Motions of Cable - Driven Parallel Robots Based on a Nonlinear Cable Tension Model", *Journal od Mechanisms and Robotics,* Vol. 9. No. 5.

Baklouti, S., Courteille, E., Lomoine, P., and Caro, S. (2019), "Vibration Reduction of Cable-Driven Parallel Robots through Elasto-Dynamic Model-Based Control", *Mechanism and Machine Theory*, pp. 329 - 345.

Barbazza, L., Oscari, F., Minto, S., and Rosati, G. (2017), "Trajectory Planning of a Suspended Cable Driven Parallel Robot with Reconfigurable End Effector", *Robotics and Computer-Integrated Manufacturing,* Vol. 48, pp. 1-11.

Begey, J., Cuvillon, L., Lesselier, M., Gouttefarde, M., and Gangloff, J. (2019), "Dynamic Control of Parallel Robots Driven by Flexible Cables and Actuated by Position - Controlled Winches", *IEEE Transactions on Robotics,* Vol. 35, No. 1.

Blanchet, L., and Merlet, J.-P. (2014), "Interference Detection for Cable-Driven Parallel Robots (CDPRs)", *2014 IEEE/ASME (AIM) International Conference on Advanced Intelligent Mechatronics,* Besacon, pp. 1413 – 1418.

Bosscher, P. M. (2004), *Disturbance Robustness Measures and Wrench - Feasible Workspace Generation Techniques for Cable - Driven Robots.* Thesis Ph.D. Georgia Institute of Technology, Georgia.

Bosscher, P., Riechel, A. T., and Ebert-Uphoff, I. (2006), "Wrench-Feasible Workspace Generation for Cable-Driven Robots", *IEEE Transactions on Robotics,* Vol. 22, No. 5.

Bosscher, P., Williams II, R. L., and Tummino, M. (2005), "A Concept for Rapidly - Deployable Cable Robot Search and Rescue Systems", *Proceedings of*

IDETC/CIE ASME International Design Engineering Technical Conferences and Computers and Information in Engineering Conference, California, pp. 589-598.

Bostelman, R., Albus, J., Dagalkis, N., Jacoff, A., and Gross, J. (1994), "Applications of the NIST Robocrane". *Proceedings of International Symposium on Robotics and Manufacturing*, Maui Hi, pp, 403-410.

Caro, S., and Martin, A. (2016), *Design and Modelling of Cable Driven Parallel Robots: State of the Art and Open Issues*, Lecture handout: Robotics and Mechanism, IRCCYN.

El-Ghazaly, G., Gouttefarde, M., and Creuze, V. (2014), "Adaptive Terminal Sliding Mode Control of a Redundantly-Actuated Cable-Driven Parallel Manipulator: CoGiRo" *Cable-Driven Parallel Robots. Mechanisms and Machine Science*, Vol. 32, pp. 179-200.

Gagliardini, L., Caro, S., Gouttefarde, M., and Girin, A. (2016)," Discrete Reconfiguration Planning for Cable-Driven Parallel Robots" *Mechanism and Machine Theory*, Vol 100, No. 6, pp. 313-337.

Gagliardini, L., Caro, S., Gouttefarde, M., Wegner, P., and Girin, A. (2014), "A Reconfigurable Cable-Driven Parallel Robot for Sandblasting and Painting of Large Structures", *Cable Driven Parallel Robots: Mechanism and Machine Science*, Vol, 32, pp. 275-291.

Gagliardini, L., Gouttefarde, M., and Caro, S. (2017), "Determination of a Dynamic Feasible Workspace for Cable-Driven Parallel Robots", *Springer Proceedings in Advanced Robotics*, pp. 361 – 370.

Gosselin, C. (2012), "Global Planning of Dynamically Feasible Trajectories for Three-DOF Spatial Cable-Suspended Parallel Robots", *Cable - Driven Parallel Robots. Mechanisms and Machine Science*, Vol. 12, pp. 3 - 22.

Gosselin, C. (2013), "Cable-Driven Parallel Mechanism: State of the Art", *Bulletion of JSME*, Vol 1, No.1, pp. 1-17.

Gough, V., and Whitewall, S. (1962), "Universal Tyre Test Machine", *Proceedings of FISITA 9th International Technical Congress*, pp. 117 - 137.

Hanafie, J., Nurhami, L., Caro, S., and Pramujati, B. (2018), "Design Optimization of Spatial Four Cables Suspended Cable Driven Parallel Robot for Rapid Life-Scan", *International Conference on Mechanical Engineering 2017*, Surabaya.

Handojo, V., Syamlan, A. T., Nurahmi, L., Pramujati, B., Tamara, M. N., and Wasiwitono, U. (2018), "Cable Driven Parallel Robot with Big Interference-Free Workspace", *2018 IFToMM Asian Mechanism and Machine Science*. Bengaluru.

Holland, C. S., & Cannon, D. J. (2003). *United States of America Patent No. US6826452B1*.

Hu, Y., Tao, L., Jia, J., and Lv, W. (2014), "Control and Simulation of Cable-Driven Parallel Robots in Offshore Cargo Handling", *Proceeding of the 11th World Congress on Intelligent Control and Automation*. Shenyang. pp. 2451-2455

Jung, J., Piao, J., Park, S., Park, J.-O., and Ko, S. Y. (2016), "Analysis of Cable Tension of High Speed Parallel Cable Robot: High Speed Position Tracking of Winch", *International Conference on Control, Automation and Systems (ICCAS)*, Gyeongju, pp. 1053 – 1056.

Kawamura, S., Choe, W., Tanaka, S., and Pandian, S. R. (1995), "Development of an Ultrahigh Speed Robot FALCON Using Wire Drive System", *IEEE International Conference on Robotics and Automation (ICRA)*, Nagoya, pp. 215 – 220.

Khosravi, A. M., and Taghirad, H. D. (2014a), "Robust PID Control of Fully-Constrained Cable Driven Paralle Robots", *Mechatronics*, Vol. 24,pp. 87 - 97.

Khosravi, M. A., and Taghirad, H. D. (2014b), "Dynamic Modeling and Control of Parallel Robots with Elastic Cables: Singular Pertubation Approach", *IEEE Transactions on Robotics*, Vol. 30, No.3.

Khosravi, M. A., Taghirad, H. D., and Oftadeh, R. (2013), "A Positive Tensions PID Controller for a Planar Cable Robot : An Experimental Study", *Proceeding of the 2013 RSI/ISM Intenational Conference on Robotics and Mechatronics*, Tehran, pp. 325-330.

Klafter, R. D., Chmielewski, T. A., and Negin, M. (1989), *Robotic Engineering: An Integrated Approach*. Prentice-Hall, Inc.

Kraus, W., Kessler, M., and Pott, A. (2015), "Pulley Friction Compensation for Winch-Integrated Cable Force Measurement and Verification on a Cable-Driven Parallel Robot", *IEEE International Conference on Robotics and Automation (ICRA)*, pp. 1627 – 1632.

Kraus, W., Schmidt, V., Rajendra, P., and Pott, A. (2014), "System Identification and Cable Force Control for a Cable-Driven Parallel Robot with Industrial Servo Drives", *IEEE International Conference on Robotics & Automation*, Hong Kong, pp. 5921 – 5926.

Lesellier, M., Cuvillon, L., Gangloff, J., and Gouttefarde, M. (2018), "An Active Stabilizer for Cable-Driven Parallel Robot Vibration Damping", *IEEE International Workshop on Intelligent Robots and Systems (IROS)*, Madrid, pp. 5063 – 5070.

Marvel, A. (2019), *Distribusi Tegangan dan Trajektori Dinamis pada Mobile Cable Driven Parallel Robot (M-CDPR)*, Mechanical Engineering: Final Project, Faculty of Industrial Technology, Institut Teknologi Sepuluh Nopember, Surabaya.

Merlet, J. P. (2017), "Simulation of discrete-time controlled cable - driven parallel robots on a trajectory", *IEEE Transactions on Robotics*, Vol. 33, No. 3, pp. 675 - 688.

Merlet, J. P. (2019), "Singularity of Cable-Driven Parallel Robot with Sagging Cables: Preliminary Investigation", *International Conference on Robotics and Automation*, Montreal, pp. 504-509.

Merlet, J.-P. (2015), "The Kinematics of Cable-Driven Parallel Robots with Sagging Cables: Preliminary Results", *IEEE International Conference on Robotics and Automation (ICRA)*, Seattle, pp. 1593 – 1598.

Mersi, R., Vali, S., Haghigi, M., Abbasnejad, G., and Masouleh, M. (2018), "Design and Control of a Suspended Cable-Driven Parallel Robot with Four Cables", *Proceedings of the 6th RSI Internal Conference on Robotics and Mechatronics (IcRoM 2018)*, Tehran, pp. 470 – 475.

Nguyen, D. Q., and Gouttefarde, M. (2014a), "Study of Reconfigurable Suspended Cable-Driven Parallel Robots for Airplane Maintenance", *IEEE/RSJ International Conference on Intelligent Robots and Systems*, Chicago, pp. 1682 – 1689.

Nguyen, D. Q., Gouttefarde, M., Company, O., and Pierrot, F. (2014b), "On the Analysis of Large-Dimension Reconfigurable Suspended Cable-Driven Parallel Robots", *IEEE International Conference on Robotics and Automation (ICRA)*, Hong Kong, pp. 5728 – 5735.

Nurahmi, L., Pramujati, B., Caro, S., and Hanafie, J. (2017), “Dimension Synthesis of Suspended Eight Cables - Driven Parallel Robot for Search and Rescue Operation”, *International Conference on Advanced Mechatronics, Intelligent Manufacture and Industrial Automation (ICAMIMIA),* Surabaya, pp. 237 – 241.

Oh, S.-R., and Agrawal, S. K. (2005), “Cable Suspended Planar Robot with Redundant Cables: Controllers with Positive Tension”, *IEEE Transactions on Robotics,* Vol. 21, No.3, pp. 457- 464.

Otis, M. J.-D., Nguyen-Dang, T.-L., Laliberte, T., Ouellet, D., Laurendeau, D., and Gosselin, C. (2009), “Cable Tension Control and Analysis of Reel Transparency for 6-DOF Haptic Foot Platform on a Cable-Driven Locomotion Interface” *International Journal of Mechanical and Mechatronics Engineering,* Vol. 3, No.4, pp. 442-454.

Picard, E., Caro, S., Claveau, F., and Plestan, F. (2018a), “Pulleys and Force Sensors Influence on Payload Estimation of Cable - Driven Parallel Robot”, *International Conference on Intelligent Robots and Systems,* Madrid. pp. 1429 – 1436.

Picard, E., Caro, S., Plestan, F., and Claveau, F. (2018b), “Control Solution for a Cable-Driven Parallel Robot with Highly Variable Payload”, *The ASME International Design Engineering Technical Conference & Computers and Information in Engineering Conference.* Quebec.

Pott, A. (2012), “Influence of Pulley Kinematics on Cable-Driven Parallel Robots”, *Latest Advances in Robot Kinematics,* pp. 197-204.

Pott, A., Mutherich, H., Kraus, W., Schmidt, V., Miermeister, P., Dietz, T., and Verl, A. (2013), “Cable-Driven Parallel Robots for Industrial Applications: The IPAnema System Family”, *International Symposium on Robotics (ISR),* Seoul, South Korea, pp. 1-6.

Qian, S., Zi, B., Shang, W.-W., and Xu, Q.-S. (2018), “A Review on Cable-driven Parallel Robots”, *Chinese Journal of Mechanical Engineering,* Vol. 31, No. 66.

Schmidt, V., Kraus, W., Martin, C., Jin, X., and Pott, A. (2017), “Black - Box Accuracy Compensation for a Cable - Driven Parallel Robot”, *17th International Conference on Control, Automation and Systems (ICCAS 2017),* Jeju, pp. 428 – 431.

Syamlan, A. T., Nurahmi, L., Pramujati, B., and Tamara, M. N. (2019), "Dynamic Trajectory Generation of Suspended Cable-Driven Parallel Robot", *International Conference on Mechanical Engineering (ICOME),* Jogjakarta.

Syamlan, A. T., Nurahmi, L., Tamara, M. N., and Pramujati, B. (2020), "Dynamic Trajectory Planning of Reconfigurable Suspended Cable Robot", *International Journal of Dynamics and Control,* Vol.8, No.2.

Takemura, F., Enomoto, M., Denou, K., Erbatur, K., Zweirs, U., and Tadokoro, S. (2004), "Proposition of a Human Body Search Strategy using a Cable - Driven Robot at Major Disaster", *Proceedings of 2004 IEEE/RSJ International Conference on Intelligent Robots and Systems,* Sendai, pp. 1456 – 1461.

Tanaka, M., Seguchi, Y., & Shimada, S. (1988), "Kineto-Statics of Skycam-Type Wire Transport System", *Proceedings of USA-Japan Symposium on Flexible Automation, Crossing Bridges: Advances in Flexible Automation and Robotics*.

Tempel, P., Schenelle, F., Pott, A., and Eberhard, P. (2015), "Design and Programming for Cable - Driven Parallel Robots in the German Pavilion at the EXPO 2015", *Machines,* Vol. 3, No. 3, pp. 223 - 241.

Yoon, J., Hwang, S. W., Bak, J.-H., & Park, J. (2018), "Vibration Suppression of CDPRs Based on Differential Flatness", *IEEE Conference on Control Technology and Applications (CCTA),* Copenhagen, pp. 259-264.